

University of Groningen

Erratum: Measurements of prompt charm production cross-sections in pp collisions at root s = 13 TeV (vol 03, 159, 2016)

Aaij, R.; Dufour, L.; Mulder, M; Onderwater, Cornelis; Pellegrino, Antonio; Tolk, S.; LHCb Collaboration

Published in:
Journal of High Energy Physics

DOI:
[10.1007/JHEP05\(2017\)074](https://doi.org/10.1007/JHEP05(2017)074)

IMPORTANT NOTE: You are advised to consult the publisher's version (publisher's PDF) if you wish to cite from it. Please check the document version below.

Document Version
Publisher's PDF, also known as Version of record

Publication date:
2017

[Link to publication in University of Groningen/UMCG research database](#)

Citation for published version (APA):

LHCb Collaboration (2017). Erratum: Measurements of prompt charm production cross-sections in pp collisions at root s = 13 TeV (vol 03, 159, 2016). Journal of High Energy Physics, 2017, [74]. DOI: 10.1007/JHEP05(2017)074

Copyright

Other than for strictly personal use, it is not permitted to download or to forward/distribute the text or part of it without the consent of the author(s) and/or copyright holder(s), unless the work is under an open content license (like Creative Commons).

Take-down policy

If you believe that this document breaches copyright please contact us providing details, and we will remove access to the work immediately and investigate your claim.

Downloaded from the University of Groningen/UMCG research database (Pure): <http://www.rug.nl/research/portal>. For technical reasons the number of authors shown on this cover page is limited to 10 maximum.

Erratum 2: Measurements of prompt charm production cross-sections in pp collisions at $\sqrt{s} = 13$ TeV



The LHCb collaboration

E-mail: alex.pearce@cern.ch

ERRATUM TO: [JHEP03\(2016\)159](#)

ARXIV EPRINT: [1510.01707](#)

An issue has been identified in the simulated samples used to calculate the efficiencies, which affects the published cross-section measurements from pp collisions at $\sqrt{s} = 13$ TeV [1]. What follows is a brief description of the nature of the problems, before the corrected results are given.

The charge collected in the LHCb VELO sensors is affected by radiation damage. One such effect, which is more pronounced in the outer regions of downstream sensors, arises from charge induction on second metal layer routing lines [2]. Prior to the start of Run 2, modifications were made to the digitization step in the LHCb simulation framework to model this effect. An error was made in the parametric implementation resulting in a reduction of the track reconstruction efficiency in simulation compared to data for tracks with low pseudorapidity. The tracking efficiency calibration procedure that was applied in this paper to the data and simulation [3] was unable to correct the mismodelling.

All results presented in the paper are affected and a similar pattern is seen for all four different mesons. The corrected cross-sections are generally lower with the largest difference at low rapidities and almost no change at high rapidities.

The corrected inclusive cross-sections for the four mesons, including charge conjugation, within the range of $1 < p_T < 8$ GeV/c are:

$$\begin{aligned}\sigma(pp \rightarrow D^0 X) &= 2072 \pm 2 \pm 124 \text{ } \mu\text{b}, \\ \sigma(pp \rightarrow D^+ X) &= 834 \pm 2 \pm 78 \text{ } \mu\text{b}, \\ \sigma(pp \rightarrow D_s^+ X) &= 353 \pm 9 \pm 76 \text{ } \mu\text{b}, \\ \sigma(pp \rightarrow D^{*+} X) &= 784 \pm 4 \pm 87 \text{ } \mu\text{b},\end{aligned}$$

The estimated $c\bar{c}$ cross-section is:

$$\sigma(pp \rightarrow c\bar{c} X)_{p_T < 8 \text{ GeV}/c, 2.0 < y < 4.5} = 2369 \pm 3 \pm 152 \pm 118 \text{ } \mu\text{b}.$$

All tables and figures in which the measurements are affected are given below, with the numbering and captions being identical to those in the original paper. The corrected 13 over 7 TeV ratios, shown in figure 7, are now in good agreement with the predictions. The 7 TeV integrated $c\bar{c}$ cross-section scaled by a predicted factor is now also in agreement with the measured cross-section at 13 TeV. Therefore, the statements made in the paragraph beginning “The data are consistently above...” and the paragraph beginning “The absolute predictions for the...”, each towards the end of section 7, are no longer supported. The exception is the sentence beginning “The measurements are consistent with...” in the latter paragraph, which is still justified.

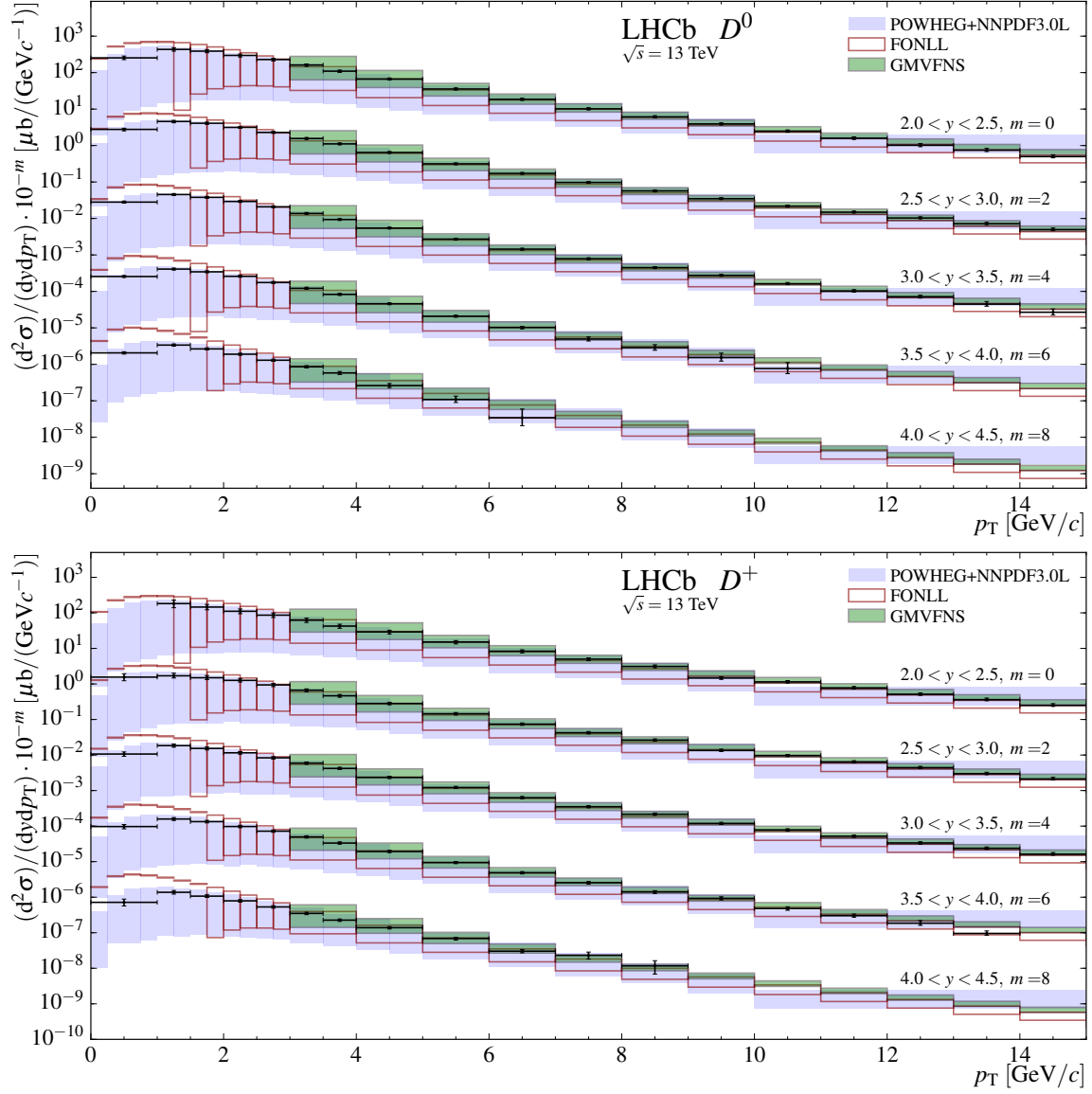


Figure 5. Measurements and predictions for the absolute prompt (top) D^0 , and (bottom) D^+ cross-sections at $\sqrt{s} = 13$ TeV. Each set of measurements and predictions in a given rapidity bin is offset by a multiplicative factor 10^{-m} , where the factor m is shown on the plots. The boxes indicate the $\pm 1\sigma$ uncertainty band on the theory predictions. In cases where this band spans more than two orders of magnitude only its upper edge is indicated.

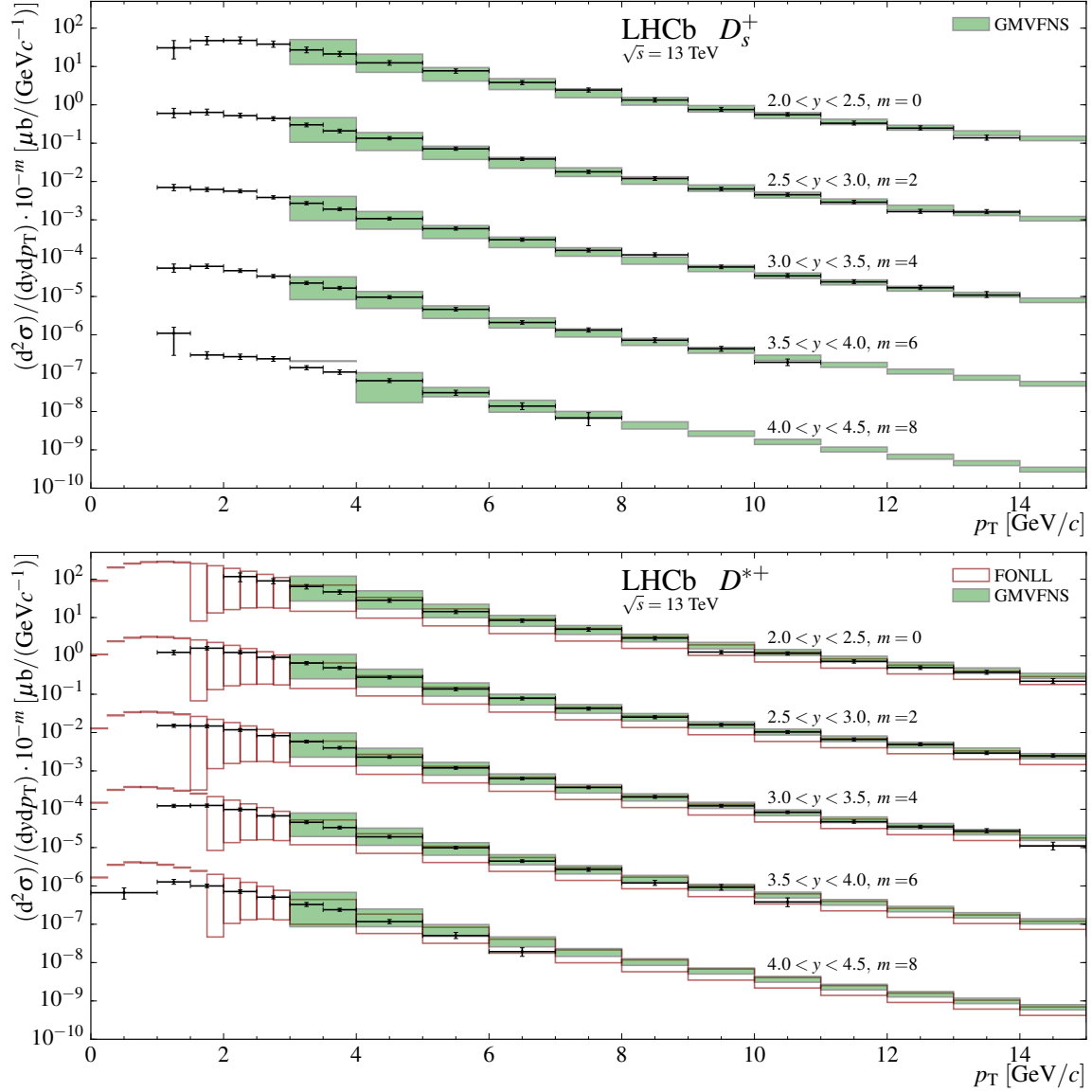


Figure 6. Measurements and predictions for the absolute prompt (top) D_s^+ , and (bottom) D^{*+} cross-sections at $\sqrt{s} = 13$ TeV. Each set of measurements and predictions in a given rapidity bin is offset by a multiplicative factor 10^{-m} , where the factor m is shown on the plots. The boxes indicate the $\pm 1\sigma$ uncertainty band on the theory predictions. In cases where this band spans more than two orders of magnitude only its upper edge is indicated.

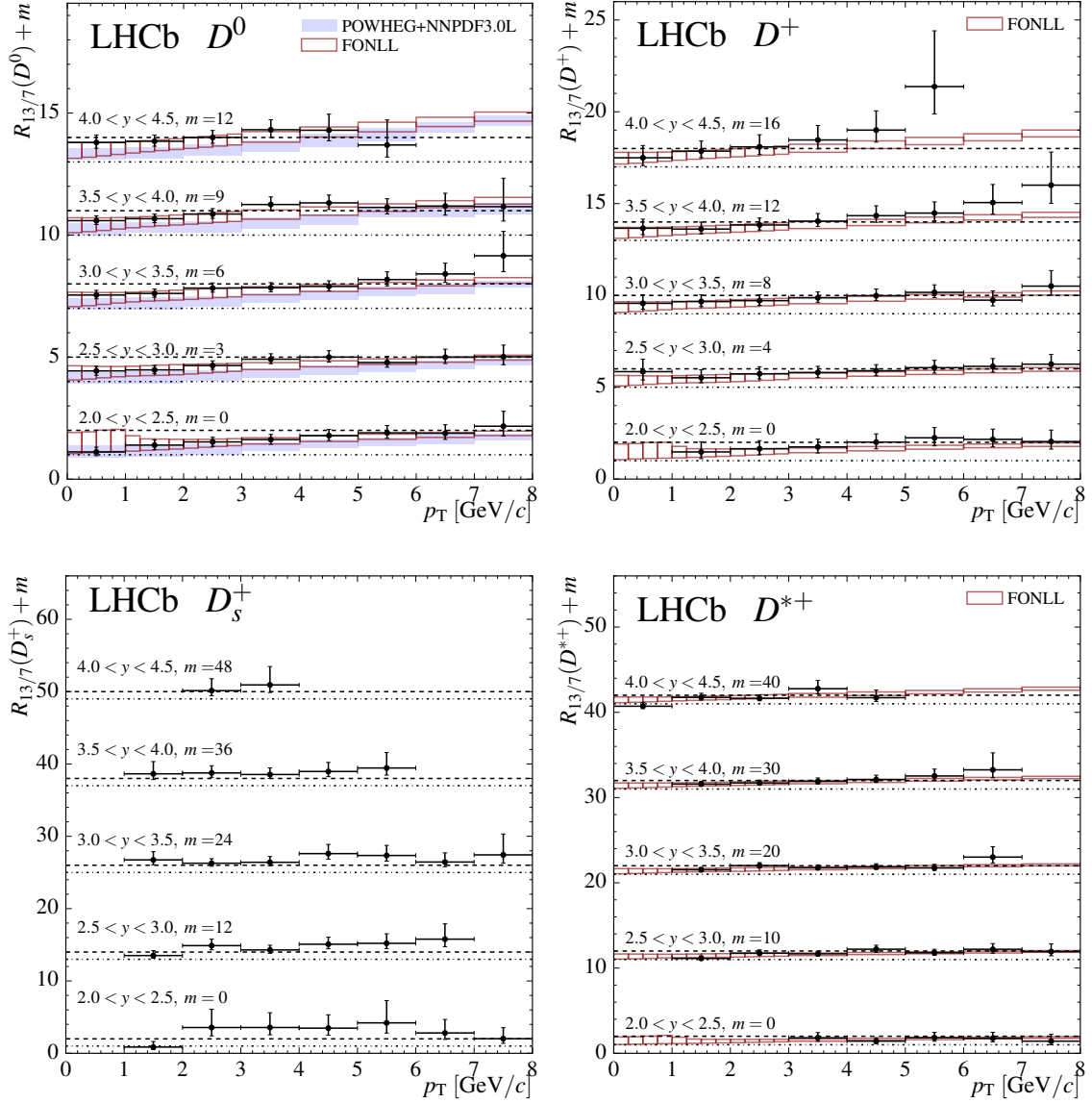


Figure 7. Measurements and predictions of the prompt D^0 , D^+ , D_s^+ , and D^{*+} cross-section ratios. The dash-dotted lines indicate the unit ratio for each of the rapidity intervals and the dashed lines indicate a ratio of two. Each set of measurements and predictions in a given rapidity bin is offset by an additive constant m , which is shown on the plot. No prediction is available for the D_s^+ ratio.

	Uncertainties (%)				Correlations (%)	
	D^0	D^+	D_s^+	D^{*+}	Bins	Modes
Luminosity			3.9		100	100
Tracking	3–10	4–14	4–14	5–11	90–100	90–100
Branching fractions	1.2	2.1	5.8	1.5	100	0–95
Simulation sample size	1–26	1–39	1–55	1–23	0	0
Simulation modelling	1	1	0.2	0.9	0	0
PID sample size	0–2	0–1	0–2	0–1	0–100	0–100
PID binning	0–44	0–10	0–20	0–15	100	100
PDF shapes	1–6	1–5	1–2	1–2	—	—

Table 2. Systematic uncertainties expressed as fractions of the cross-section measurements, in percent. Uncertainties that are computed bin-by-bin are expressed as ranges giving the minimum to maximum values. Ranges for the correlations between p_T - y bins and between modes are also given, expressed in percent.

			Extrapolation factor	Cross-section (μb)
D^0	$0 < p_T < 8 \text{ GeV}/c$	$2 < y < 4.5$	1.0014 ± 0.0024	$2709 \pm 2 \pm 165$
D^+	$0 < p_T < 8 \text{ GeV}/c$	$2 < y < 4.5$	1.049 ± 0.031	$1102 \pm 5 \pm 111$
D^0	$1 < p_T < 8 \text{ GeV}/c$	$2 < y < 4.5$	1.0018 ± 0.0025	$2072 \pm 2 \pm 124$
D^+	$1 < p_T < 8 \text{ GeV}/c$	$2 < y < 4.5$	—	$834 \pm 2 \pm 78$
D_s^+	$1 < p_T < 8 \text{ GeV}/c$	$2 < y < 4.5$	—	$353 \pm 9 \pm 76$
D^{*+}	$1 < p_T < 8 \text{ GeV}/c$	$2 < y < 4.5$	1.102 ± 0.081	$784 \pm 4 \pm 87$
D^0	$0 < p_T < 8 \text{ GeV}/c$	$2.5 < y < 4$	—	$1720 \pm 1 \pm 98$
D^+	$0 < p_T < 8 \text{ GeV}/c$	$2.5 < y < 4$	—	$706 \pm 4 \pm 66$
D^0	$1 < p_T < 8 \text{ GeV}/c$	$2.5 < y < 4$	—	$1313 \pm 1 \pm 73$
D^+	$1 < p_T < 8 \text{ GeV}/c$	$2.5 < y < 4$	—	$527 \pm 1 \pm 45$
D_s^+	$1 < p_T < 8 \text{ GeV}/c$	$2.5 < y < 4$	—	$227 \pm 2 \pm 24$
D^{*+}	$1 < p_T < 8 \text{ GeV}/c$	$2.5 < y < 4$	—	$493 \pm 2 \pm 41$

Table 3. Prompt charm production cross-sections in the kinematic ranges given. The computation of the extrapolation factors is described in the text. The first uncertainty on the cross-section is statistical, and the second is systematic and includes the contribution from the extrapolation factor. No extrapolation factor is given for $D^+_{(s)}$ as a measurement is available in every bin of the integrated phase space.

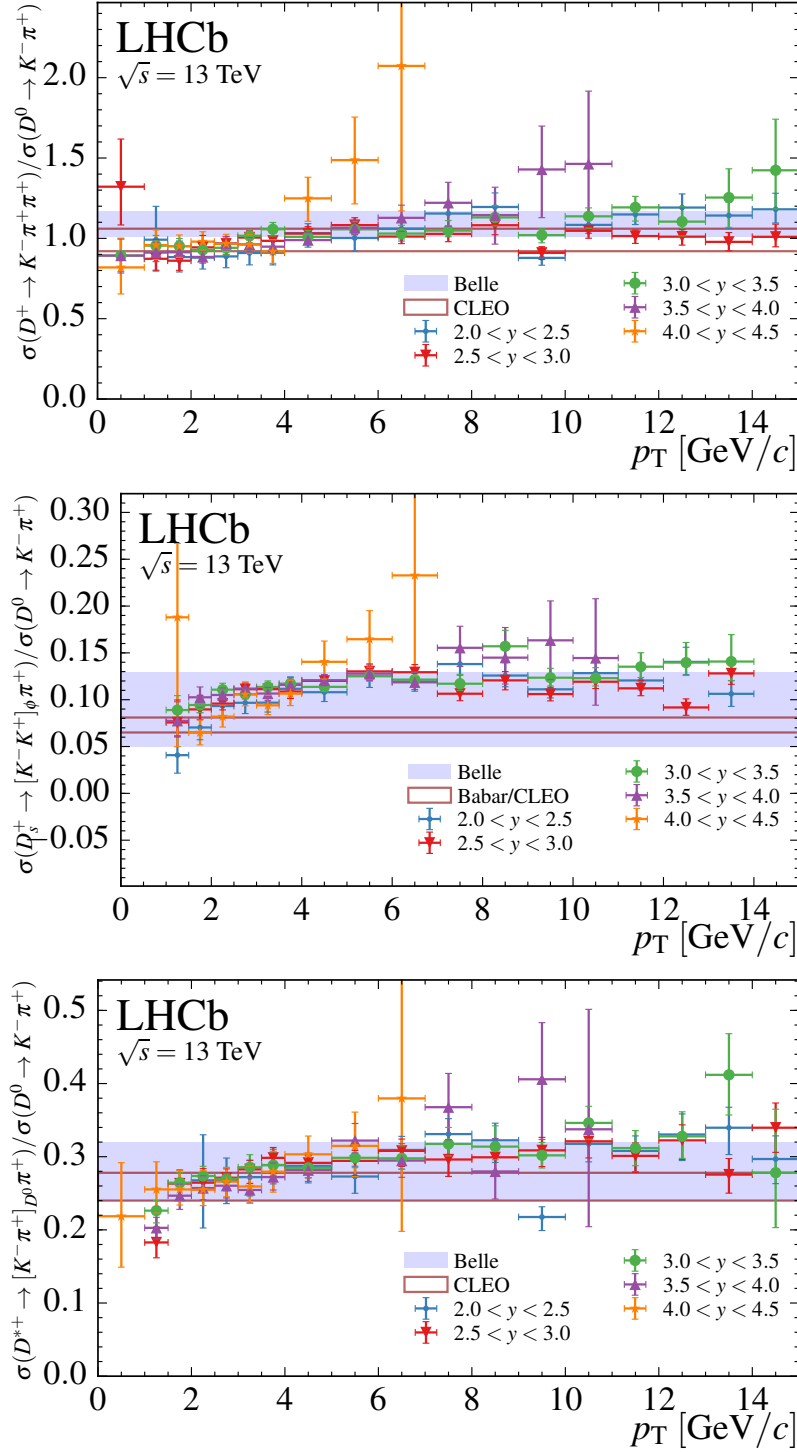


Figure 8. Ratios of cross-section-times-branching-fraction measurements of (top) D^+ , (middle) D_s^+ , and (bottom) D^{*+} mesons with respect to the D^0 measurements. The bands indicate the corresponding ratios computed using measurements from e^+e^- collider experiments [39–41]. The ratios are given as a function of p_T and different symbols indicate different ranges in y . The notation $\sigma(D \rightarrow f)$ is shorthand for $\sigma(D) \times \mathcal{B}(D \rightarrow f)$.

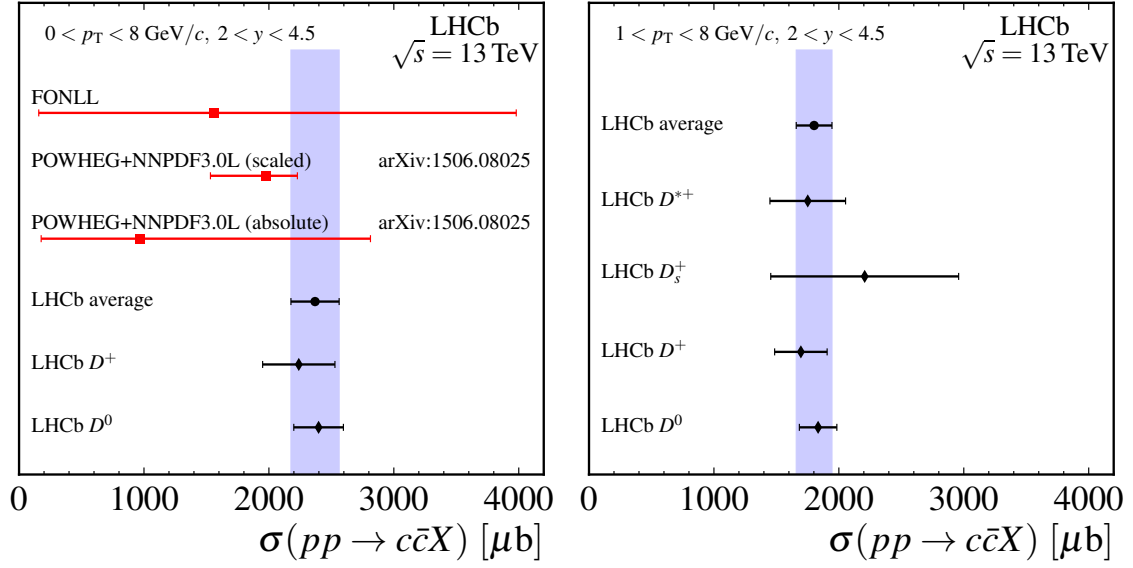


Figure 9. Integrated cross-sections (black diamonds), their average (black circle and blue band) and theory predictions (red squares) [1, 2] are shown (left) based on the D^0 and D^+ for $0 < p_T < 8$ GeV/c and (right) for measurements based on all four mesons for $1 < p_T < 8$ GeV/c. The “absolute” predictions are based on calculations of the 13 TeV cross-section, while the “scaled” predictions are based on calculations of the 13 to 7 TeV ratio multiplied with the LHCb measurement at 7 TeV [16].

Quantity	Measurement
$\sigma(D^+ \rightarrow K^- \pi^+ \pi^+)/\sigma(D^0 \rightarrow K^- \pi^+)$	$0.950^{+0.003+0.040}_{-0.003-0.040}$
$\sigma(D_s^+ \rightarrow [K^- K^+]_\phi \pi^+)/\sigma(D^0 \rightarrow K^- \pi^+)$	$0.0991^{+0.0026+0.0053}_{-0.0026-0.0079}$
$\sigma(D^{*+} \rightarrow [K^- \pi^+]_{D^0} \pi^+)/\sigma(D^0 \rightarrow K^- \pi^+)$	$0.256^{+0.001+0.021}_{-0.001-0.021}$
$\sigma(D_s^+ \rightarrow [K^- K^+]_\phi \pi^+)/\sigma(D^+ \rightarrow K^- \pi^+ \pi^+)$	$0.1043^{+0.0028+0.0038}_{-0.0028-0.0066}$
$\sigma(D^{*+} \rightarrow [K^- \pi^+]_{D^0} \pi^+)/\sigma(D^+ \rightarrow K^- \pi^+ \pi^+)$	$0.270^{+0.002+0.023}_{-0.002-0.022}$
$\sigma(D_s^+ \rightarrow [K^- K^+]_\phi \pi^+)/\sigma(D^{*+} \rightarrow [K^- \pi^+]_{D^0} \pi^+)$	$0.390^{+0.010+0.038}_{-0.010-0.045}$

Table 4. Ratios of integrated cross-section-times-branching-fraction measurements in the kinematic range $1 < p_T < 8$ GeV/c and $2 < y < 4.5$. The first uncertainty on the ratio is statistical and the second is systematic. The notation $\sigma(D \rightarrow f)$ is shorthand for $\sigma(D) \times \mathcal{B}(D \rightarrow f)$.

p_T [MeV/c]	y				
	[2, 2.5]	[2.5, 3]	[3, 3.5]	[3.5, 4]	[4, 4.5]
[0, 1000]	254^{+2}_{-2}	$277.3^{+1.0}_{-1.0}$	$281.1^{+0.9}_{-0.9}$	256^{+1}_{-1}	206^{+2}_{-2}
[1000, 1500]	433^{+3}_{-3}	457^{+2}_{-2}	454^{+1}_{-1}	409^{+2}_{-2}	337^{+3}_{-3}
[1500, 2000]	388^{+2}_{-2}	409^{+1}_{-1}	380^{+1}_{-1}	344^{+1}_{-1}	265^{+2}_{-2}
[2000, 2500]	296^{+2}_{-2}	$314.4^{+1.0}_{-1.0}$	$292.5^{+0.9}_{-0.9}$	259^{+1}_{-1}	190^{+2}_{-2}
[2500, 3000]	228^{+1}_{-1}	$228.9^{+0.7}_{-0.7}$	$208.8^{+0.7}_{-0.7}$	$175.0^{+0.8}_{-0.8}$	$129.6^{+1.2}_{-1.2}$
[3000, 3500]	$161.3^{+0.9}_{-0.9}$	$156.1^{+0.5}_{-0.5}$	$137.3^{+0.5}_{-0.5}$	$121.4^{+0.6}_{-0.6}$	$85.6^{+0.9}_{-0.9}$
[3500, 4000]	$109.7^{+0.6}_{-0.6}$	$111.0^{+0.4}_{-0.4}$	$93.5^{+0.4}_{-0.4}$	$82.7^{+0.4}_{-0.4}$	$58.0^{+0.8}_{-0.8}$
[4000, 5000]	$66.5^{+0.3}_{-0.3}$	$64.5^{+0.2}_{-0.2}$	$54.5^{+0.2}_{-0.2}$	$45.9^{+0.2}_{-0.2}$	$26.1^{+0.4}_{-0.4}$
[5000, 6000]	$35.5^{+0.2}_{-0.2}$	$31.5^{+0.1}_{-0.1}$	$27.1^{+0.1}_{-0.1}$	$20.8^{+0.1}_{-0.1}$	$10.9^{+0.4}_{-0.4}$
[6000, 7000]	$18.5^{+0.1}_{-0.1}$	$17.20^{+0.09}_{-0.09}$	$14.40^{+0.09}_{-0.09}$	$10.20^{+0.12}_{-0.12}$	$3.4^{+0.5}_{-0.5}$
[7000, 8000]	$10.15^{+0.09}_{-0.09}$	$9.71^{+0.07}_{-0.07}$	$7.88^{+0.07}_{-0.07}$	$4.94^{+0.10}_{-0.10}$	
[8000, 9000]	$6.11^{+0.07}_{-0.07}$	$5.72^{+0.05}_{-0.05}$	$4.49^{+0.05}_{-0.05}$	$2.88^{+0.11}_{-0.11}$	
[9000, 10000]	$3.92^{+0.06}_{-0.06}$	$3.48^{+0.04}_{-0.04}$	$2.75^{+0.04}_{-0.04}$	$1.53^{+0.11}_{-0.11}$	
[10000, 11000]	$2.48^{+0.05}_{-0.05}$	$2.18^{+0.03}_{-0.03}$	$1.62^{+0.04}_{-0.04}$	$0.77^{+0.13}_{-0.13}$	
[11000, 12000]	$1.59^{+0.04}_{-0.04}$	$1.49^{+0.03}_{-0.03}$	$1.025^{+0.034}_{-0.034}$		
[12000, 13000]	$1.01^{+0.03}_{-0.03}$	$1.031^{+0.026}_{-0.026}$	$0.716^{+0.034}_{-0.034}$		
[13000, 14000]	$0.746^{+0.026}_{-0.026}$	$0.718^{+0.023}_{-0.023}$	$0.447^{+0.031}_{-0.031}$		
[14000, 15000]	$0.498^{+0.022}_{-0.022}$	$0.495^{+0.020}_{-0.020}$	$0.268^{+0.031}_{-0.031}$		

Table 5. Differential production cross-sections, $d^2\sigma/(dp_T dy)$, in pb/(GeV/c) for prompt $D^0 + \bar{D}^0$ mesons in bins of (p_T, y) . The first uncertainty is statistical, and the second is the total systematic.

p_T [MeV/c]	y									
	[2, 2.5]	[2.5, 3]		[3, 3.5]		[3.5, 4]		[4, 4.5]		
[0, 1000]		156 \pm 6 $^{+}$ 6 $^{-}$	38 \pm 32 $^{+}$ 32 $^{-}$	107 \pm 3 $^{+}$ 3 $^{-}$	15 \pm 14 $^{+}$ 14 $^{-}$	97 \pm 3 $^{+}$ 3 $^{-}$	13 \pm 13 $^{+}$ 13 $^{-}$	72 \pm 5 $^{+}$ 5 $^{-}$	16 \pm 14 $^{+}$ 14 $^{-}$	
[1000, 1500]	182 \pm 7 $^{+}$ 7 $^{-}$	47 \pm 42 $^{+}$ 42 $^{-}$	2 \pm 31 $^{+}$ 22 $^{-}$	184 \pm 1 $^{+}$ 1 $^{-}$	19 \pm 18 $^{+}$ 18 $^{-}$	158 \pm 2 $^{+}$ 2 $^{-}$	15 \pm 15 $^{+}$ 14 $^{-}$	137 \pm 3 $^{+}$ 3 $^{-}$	16 \pm 15 $^{+}$ 15 $^{-}$	
[1500, 2000]	146 \pm 2 $^{+}$ 2 $^{-}$	27 \pm 23 $^{+}$ 23 $^{-}$	8 \pm 23.0 $^{+}$ 16.6 $^{-}$	153.5 \pm 0.7 $^{+}$ 0.7 $^{-}$	13.7 \pm 14.2 $^{+}$ 14.2 $^{-}$	133.6 \pm 0.7 $^{+}$ 0.7 $^{-}$	11.4 \pm 10.4 $^{+}$ 10.4 $^{-}$	107.1 \pm 1.2 $^{+}$ 1.2 $^{-}$	9.6 \pm 9.1 $^{+}$ 9.1 $^{-}$	
[2000, 2500]	111 \pm 1 $^{+}$ 1 $^{-}$	18 \pm 16 $^{+}$ 16 $^{-}$	5 \pm 16.4 $^{+}$ 12.9 $^{-}$	115.4 \pm 0.4 $^{+}$ 0.4 $^{-}$	9.5 \pm 9.7 $^{+}$ 9.7 $^{-}$	97.4 \pm 0.4 $^{+}$ 0.4 $^{-}$	7.8 \pm 7.2 $^{+}$ 7.2 $^{-}$	78.9 \pm 0.7 $^{+}$ 0.7 $^{-}$	6.3 \pm 6.1 $^{+}$ 6.1 $^{-}$	
[2500, 3000]	86.1 \pm 0.7 $^{+}$ 0.7 $^{-}$	13.1 \pm 12.3 $^{+}$ 12.3 $^{-}$	8.8 \pm 10.0 $^{+}$ 10.0 $^{-}$	83.5 \pm 0.3 $^{+}$ 0.3 $^{-}$	6.5 \pm 6.5 $^{+}$ 6.5 $^{-}$	72.1 \pm 0.3 $^{+}$ 0.3 $^{-}$	5.4 \pm 5.1 $^{+}$ 5.1 $^{-}$	53.2 \pm 0.4 $^{+}$ 0.4 $^{-}$	4.4 \pm 4.0 $^{+}$ 4.0 $^{-}$	
[3000, 3500]	62.3 \pm 0.5 $^{+}$ 0.5 $^{-}$	8.8 \pm 8.6 $^{+}$ 8.6 $^{-}$	6.0 \pm 6.6 $^{+}$ 6.6 $^{-}$	59.3 \pm 0.2 $^{+}$ 0.2 $^{-}$	4.6 \pm 4.3 $^{+}$ 4.3 $^{-}$	49.7 \pm 0.2 $^{+}$ 0.2 $^{-}$	3.8 \pm 3.4 $^{+}$ 3.4 $^{-}$	35.0 \pm 0.3 $^{+}$ 0.3 $^{-}$	2.7 \pm 2.7 $^{+}$ 2.7 $^{-}$	
[3500, 4000]	42.4 \pm 0.3 $^{+}$ 0.3 $^{-}$	5.5 \pm 5.6 $^{+}$ 5.6 $^{-}$	4.2 \pm 4.2 $^{+}$ 4.2 $^{-}$	42.0 \pm 0.2 $^{+}$ 0.2 $^{-}$	3.3 \pm 2.9 $^{+}$ 2.9 $^{-}$	33.3 \pm 0.2 $^{+}$ 0.2 $^{-}$	2.7 \pm 2.2 $^{+}$ 2.2 $^{-}$	22.6 \pm 0.2 $^{+}$ 0.2 $^{-}$	1.7 \pm 1.8 $^{+}$ 1.8 $^{-}$	
[4000, 5000]	29.2 \pm 0.2 $^{+}$ 0.2 $^{-}$	3.2 \pm 3.7 $^{+}$ 3.7 $^{-}$	2.35 \pm 2.34 $^{+}$ 2.34 $^{-}$	23.36 \pm 0.08 $^{+}$ 0.08 $^{-}$	1.83 \pm 1.48 $^{+}$ 1.48 $^{-}$	19.29 \pm 0.08 $^{+}$ 0.08 $^{-}$	1.51 \pm 1.26 $^{+}$ 1.26 $^{-}$	13.9 \pm 0.1 $^{+}$ 0.1 $^{-}$	0.9 \pm 1.1 $^{+}$ 1.1 $^{-}$	
[5000, 6000]	15.1 \pm 0.1 $^{+}$ 0.1 $^{-}$	1.5 \pm 1.7 $^{+}$ 1.7 $^{-}$	1.18 \pm 1.10 $^{+}$ 1.10 $^{-}$	12.18 \pm 0.05 $^{+}$ 0.05 $^{-}$	0.94 \pm 0.78 $^{+}$ 0.78 $^{-}$	9.44 \pm 0.05 $^{+}$ 0.05 $^{-}$	0.71 \pm 0.63 $^{+}$ 0.63 $^{-}$	6.87 \pm 0.11 $^{+}$ 0.11 $^{-}$	0.60 \pm 0.64 $^{+}$ 0.64 $^{-}$	
[6000, 7000]	8.34 \pm 0.07 $^{+}$ 0.07 $^{-}$	0.76 \pm 0.84 $^{+}$ 0.84 $^{-}$	0.59 \pm 0.54 $^{+}$ 0.54 $^{-}$	6.30 \pm 0.04 $^{+}$ 0.04 $^{-}$	0.49 \pm 0.40 $^{+}$ 0.40 $^{-}$	4.89 \pm 0.04 $^{+}$ 0.04 $^{-}$	0.32 \pm 0.37 $^{+}$ 0.37 $^{-}$	3.03 \pm 0.09 $^{+}$ 0.09 $^{-}$	0.30 \pm 0.30 $^{+}$ 0.30 $^{-}$	
[7000, 8000]	4.98 \pm 0.05 $^{+}$ 0.05 $^{-}$	0.47 \pm 0.46 $^{+}$ 0.46 $^{-}$	0.33 \pm 0.31 $^{+}$ 0.31 $^{-}$	3.51 \pm 0.03 $^{+}$ 0.03 $^{-}$	0.28 \pm 0.23 $^{+}$ 0.23 $^{-}$	2.56 \pm 0.03 $^{+}$ 0.03 $^{-}$	0.18 \pm 0.21 $^{+}$ 0.21 $^{-}$	2.31 \pm 0.13 $^{+}$ 0.13 $^{-}$	0.53 \pm 0.47 $^{+}$ 0.47 $^{-}$	
[8000, 9000]	3.11 \pm 0.04 $^{+}$ 0.04 $^{-}$	0.31 \pm 0.25 $^{+}$ 0.25 $^{-}$	0.21 \pm 0.19 $^{+}$ 0.19 $^{-}$	2.16 \pm 0.02 $^{+}$ 0.02 $^{-}$	0.17 \pm 0.14 $^{+}$ 0.14 $^{-}$	1.40 \pm 0.02 $^{+}$ 0.02 $^{-}$	0.12 \pm 0.13 $^{+}$ 0.13 $^{-}$	1.17 \pm 0.09 $^{+}$ 0.09 $^{-}$	0.46 \pm 0.47 $^{+}$ 0.47 $^{-}$	
[9000, 10000]	1.46 \pm 0.02 $^{+}$ 0.02 $^{-}$	0.13 \pm 0.11 $^{+}$ 0.11 $^{-}$	0.11 \pm 0.09 $^{+}$ 0.09 $^{-}$	1.192 \pm 0.015 $^{+}$ 0.015 $^{-}$	0.83 \pm 0.083 $^{+}$ 0.083 $^{-}$	0.928 \pm 0.025 $^{+}$ 0.025 $^{-}$	0.096 \pm 0.087 $^{+}$ 0.087 $^{-}$			
[10000, 11000]	1.144 \pm 0.020 $^{+}$ 0.020 $^{-}$	0.098 \pm 0.081 $^{+}$ 0.081 $^{-}$	0.072 \pm 0.061 $^{+}$ 0.061 $^{-}$	0.784 \pm 0.013 $^{+}$ 0.013 $^{-}$	0.050 \pm 0.052 $^{+}$ 0.052 $^{-}$	0.477 \pm 0.020 $^{+}$ 0.020 $^{-}$	0.057 \pm 0.044 $^{+}$ 0.044 $^{-}$			
[11000, 12000]	0.774 \pm 0.016 $^{+}$ 0.016 $^{-}$	0.070 \pm 0.054 $^{+}$ 0.054 $^{-}$	0.050 \pm 0.037 $^{+}$ 0.037 $^{-}$	0.520 \pm 0.011 $^{+}$ 0.011 $^{-}$	0.035 \pm 0.034 $^{+}$ 0.034 $^{-}$	0.301 \pm 0.017 $^{+}$ 0.017 $^{-}$	0.031 \pm 0.021 $^{+}$ 0.021 $^{-}$			
[12000, 13000]	0.513 \pm 0.012 $^{+}$ 0.012 $^{-}$	0.049 \pm 0.033 $^{+}$ 0.033 $^{-}$	0.036 \pm 0.025 $^{+}$ 0.025 $^{-}$	0.336 \pm 0.009 $^{+}$ 0.009 $^{-}$	0.024 \pm 0.021 $^{+}$ 0.021 $^{-}$	0.185 \pm 0.011 $^{+}$ 0.011 $^{-}$	0.034 \pm 0.021 $^{+}$ 0.021 $^{-}$			
[13000, 14000]	0.362 \pm 0.010 $^{+}$ 0.010 $^{-}$	0.037 \pm 0.023 $^{+}$ 0.023 $^{-}$	0.028 \pm 0.015 $^{+}$ 0.015 $^{-}$	0.238 \pm 0.008 $^{+}$ 0.008 $^{-}$	0.019 \pm 0.014 $^{+}$ 0.014 $^{-}$	0.096 \pm 0.009 $^{+}$ 0.009 $^{-}$	0.015 \pm 0.006 $^{+}$ 0.006 $^{-}$			
[14000, 15000]	0.250 \pm 0.008 $^{+}$ 0.008 $^{-}$	0.028 \pm 0.014 $^{+}$ 0.014 $^{-}$	0.022 \pm 0.009 $^{+}$ 0.009 $^{-}$	0.162 \pm 0.007 $^{+}$ 0.007 $^{-}$	0.017 \pm 0.007 $^{+}$ 0.007 $^{-}$					

Table 6. Differential production cross-sections, $d^2\sigma/(dp_T dy)$, in pb/(GeV/c) for prompt $D^+ + D^-$ mesons in bins of (p_T, y) . The first uncertainty is statistical, and the second is the total systematic.

p_T [MeV/c]	y									
	[2, 2.5]		[2.5, 3]		[3, 3.5]		[3.5, 4]		[4, 4.5]	
[1000, 1500]	31^{+8}_{-8}	15^{+13}_{-13}	60^{+4}_{-4}	21^{+13}_{-13}	70^{+4}_{-4}	13^{+13}_{-13}	55^{+5}_{-5}	14^{+14}_{-11}	110^{+36}_{-36}	34^{+72}_{-72}
[1500, 2000]	47^{+3}_{-3}	13^{+10}_{-10}	63^{+2}_{-2}	14^{+10}_{-10}	$62.1^{+1.6}_{-1.6}$	$7.5^{+7.5}_{-7.2}$	$61.2^{+2.2}_{-2.2}$	$8.5^{+8.5}_{-7.2}$	$29.8^{+3.1}_{-3.1}$	$5.9^{+5.9}_{-5.5}$
[2000, 2500]	48^{+2}_{-2}	11^{+9}_{-9}	$52.2^{+0.9}_{-0.9}$	$8.4^{+5.8}_{-5.8}$	$56.1^{+0.9}_{-0.9}$	$6.2^{+5.6}_{-5.6}$	$47.1^{+1.1}_{-1.1}$	$5.3^{+4.7}_{-4.7}$	$26.9^{+1.8}_{-1.8}$	$4.2^{+3.7}_{-3.7}$
[2500, 3000]	$38.2^{+1.1}_{-1.1}$	$7.8^{+6.5}_{-6.5}$	$44.1^{+0.6}_{-0.6}$	$4.9^{+5.5}_{-5.5}$	$38.3^{+0.5}_{-0.5}$	$4.2^{+3.3}_{-3.3}$	$33.9^{+0.7}_{-0.7}$	$3.5^{+3.2}_{-3.2}$	$23.7^{+1.1}_{-1.1}$	$3.2^{+3.1}_{-3.1}$
[3000, 3500]	$27.1^{+0.7}_{-0.7}$	$4.9^{+4.2}_{-4.2}$	$30.1^{+0.4}_{-0.4}$	$3.2^{+3.4}_{-3.4}$	$27.0^{+0.4}_{-0.4}$	$2.9^{+2.3}_{-2.3}$	$22.4^{+0.4}_{-0.4}$	$2.3^{+2.1}_{-2.1}$	$13.9^{+0.7}_{-0.7}$	$1.7^{+1.6}_{-1.6}$
[3500, 4000]	$21.2^{+0.5}_{-0.5}$	$3.6^{+3.0}_{-3.0}$	$20.9^{+0.3}_{-0.3}$	$2.2^{+2.2}_{-2.2}$	$19.0^{+0.3}_{-0.3}$	$2.0^{+1.6}_{-1.6}$	$16.6^{+0.3}_{-0.3}$	$1.7^{+1.5}_{-1.5}$	$10.7^{+0.6}_{-0.6}$	$1.5^{+1.3}_{-1.3}$
[4000, 5000]	$12.4^{+0.2}_{-0.2}$	$1.8^{+1.6}_{-1.6}$	$13.4^{+0.2}_{-0.2}$	$1.4^{+1.3}_{-1.3}$	$10.7^{+0.1}_{-0.1}$	$1.1^{+0.9}_{-0.9}$	$9.60^{+0.17}_{-0.17}$	$0.93^{+0.87}_{-0.87}$	$6.36^{+0.28}_{-0.28}$	$0.78^{+0.61}_{-0.61}$
[5000, 6000]	$7.7^{+0.2}_{-0.2}$	$0.9^{+1.0}_{-1.0}$	$7.11^{+0.11}_{-0.11}$	$0.79^{+0.59}_{-0.59}$	$5.89^{+0.10}_{-0.10}$	$0.58^{+0.49}_{-0.49}$	$4.62^{+0.10}_{-0.10}$	$0.54^{+0.41}_{-0.41}$	$3.10^{+0.20}_{-0.20}$	$0.45^{+0.40}_{-0.40}$
[6000, 7000]	$3.83^{+0.10}_{-0.10}$	$0.44^{+0.46}_{-0.46}$	$3.85^{+0.08}_{-0.08}$	$0.41^{+0.34}_{-0.34}$	$3.03^{+0.07}_{-0.07}$	$0.31^{+0.27}_{-0.27}$	$2.10^{+0.07}_{-0.07}$	$0.25^{+0.20}_{-0.20}$	$1.39^{+0.16}_{-0.16}$	$0.21^{+0.21}_{-0.21}$
[7000, 8000]	$2.43^{+0.08}_{-0.08}$	$0.32^{+0.26}_{-0.26}$	$1.79^{+0.05}_{-0.05}$	$0.18^{+0.17}_{-0.17}$	$1.60^{+0.05}_{-0.05}$	$0.18^{+0.14}_{-0.14}$	$1.33^{+0.06}_{-0.06}$	$0.18^{+0.14}_{-0.14}$	$0.68^{+0.18}_{-0.18}$	$0.18^{+0.18}_{-0.18}$
[8000, 9000]	$1.33^{+0.05}_{-0.05}$	$0.17^{+0.14}_{-0.14}$	$1.19^{+0.04}_{-0.04}$	$0.13^{+0.12}_{-0.12}$	$1.22^{+0.04}_{-0.04}$	$0.16^{+0.12}_{-0.12}$	$0.72^{+0.05}_{-0.05}$	$0.10^{+0.09}_{-0.09}$		
[9000, 10000]	$0.754^{+0.036}_{-0.036}$	$0.097^{+0.067}_{-0.067}$	$0.639^{+0.026}_{-0.026}$	$0.069^{+0.054}_{-0.054}$	$0.588^{+0.027}_{-0.027}$	$0.066^{+0.050}_{-0.050}$	$0.433^{+0.041}_{-0.041}$	$0.053^{+0.044}_{-0.044}$		
[10000, 11000]	$0.553^{+0.032}_{-0.032}$	$0.063^{+0.037}_{-0.037}$	$0.450^{+0.023}_{-0.023}$	$0.045^{+0.031}_{-0.031}$	$0.346^{+0.022}_{-0.022}$	$0.043^{+0.023}_{-0.023}$	$0.192^{+0.033}_{-0.033}$	$0.025^{+0.010}_{-0.010}$		
[11000, 12000]	$0.331^{+0.025}_{-0.025}$	$0.038^{+0.023}_{-0.023}$	$0.289^{+0.018}_{-0.018}$	$0.031^{+0.017}_{-0.017}$	$0.240^{+0.018}_{-0.018}$	$0.028^{+0.012}_{-0.012}$				
[12000, 13000]	$0.247^{+0.020}_{-0.020}$	$0.030^{+0.016}_{-0.016}$	$0.164^{+0.014}_{-0.014}$	$0.020^{+0.008}_{-0.008}$	$0.169^{+0.016}_{-0.016}$	$0.022^{+0.006}_{-0.006}$				
[13000, 14000]	$0.137^{+0.016}_{-0.016}$	$0.019^{+0.009}_{-0.009}$	$0.159^{+0.014}_{-0.014}$	$0.022^{+0.006}_{-0.006}$	$0.1090^{+0.0146}_{-0.0146}$	$0.0212^{+0.0010}_{-0.0010}$				
[14000, 15000]										

Table 7. Differential production cross-sections, $d^2\sigma/(dp_T dy)$, in $\mu\text{b}/(\text{GeV}/c)$ for prompt $D_s^+ + D_s^-$ mesons in bins of (p_T, y) . The first uncertainty is statistical, and the second is the total systematic.

p_T [MeV/c]	y				
	[2, 2.5]	[2.5, 3]	[3, 3.5]	[3.5, 4]	[4, 4.5]
[0, 1000]					$67^{+9}_{-9} \text{ }^{20}_{-19}$
[1000, 1500]		$124^{+5}_{-5} \text{ }^{16}_{-17}$	$152^{+2}_{-2} \text{ }^{13}_{-15}$	$123^{+2}_{-2} \text{ }^{12}_{-12}$	$127^{+4}_{-4} \text{ }^{20}_{-16}$
[1500, 2000]		$159^{+3}_{-3} \text{ }^{18}_{-16}$	$148^{+1}_{-1} \text{ }^{12}_{-14}$	$125^{+1}_{-1} \text{ }^{11}_{-12}$	$100^{+2}_{-2} \text{ }^{11}_{-9}$
[2000, 2500]	$117^{+11}_{-11} \text{ }^{27}_{-29}$	$123^{+1}_{-1} \text{ }^{15}_{-10}$	$118.2^{+0.8}_{-0.8} \text{ }^{9.4}_{-11.1}$	$98.4^{+0.8}_{-0.8} \text{ }^{9.2}_{-8.2}$	$71.3^{+1.3}_{-1.3} \text{ }^{8.1}_{-7.1}$
[2500, 3000]	$90^{+3}_{-3} \text{ }^{13}_{-14}$	$91.7^{+0.8}_{-0.8} \text{ }^{8.3}_{-9.3}$	$83.2^{+0.5}_{-0.5} \text{ }^{7.6}_{-6.7}$	$67.3^{+0.6}_{-0.6} \text{ }^{6.3}_{-5.6}$	$50.9^{+1.0}_{-1.0} \text{ }^{4.4}_{-4.8}$
[3000, 3500]	$64.8^{+1.6}_{-1.6} \text{ }^{7.7}_{-9.0}$	$65.2^{+0.5}_{-0.5} \text{ }^{5.6}_{-6.6}$	$57.9^{+0.4}_{-0.4} \text{ }^{5.4}_{-4.3}$	$45.7^{+0.4}_{-0.4} \text{ }^{4.3}_{-3.7}$	$32.8^{+0.7}_{-0.7} \text{ }^{4.2}_{-3.7}$
[3500, 4000]	$46.8^{+1.0}_{-1.0} \text{ }^{5.3}_{-6.1}$	$48.9^{+0.4}_{-0.4} \text{ }^{4.2}_{-4.9}$	$39.9^{+0.3}_{-0.3} \text{ }^{3.7}_{-2.9}$	$33.2^{+0.3}_{-0.3} \text{ }^{3.1}_{-2.7}$	$23.9^{+0.6}_{-0.6} \text{ }^{2.1}_{-2.1}$
[4000, 5000]	$28.2^{+0.4}_{-0.4} \text{ }^{2.8}_{-3.3}$	$27.8^{+0.2}_{-0.2} \text{ }^{2.3}_{-2.7}$	$22.9^{+0.1}_{-0.1} \text{ }^{2.0}_{-1.6}$	$19.1^{+0.2}_{-0.2} \text{ }^{1.8}_{-1.6}$	$11.7^{+0.3}_{-0.3} \text{ }^{1.5}_{-1.3}$
[5000, 6000]	$14.3^{+0.2}_{-0.2} \text{ }^{1.4}_{-1.6}$	$13.7^{+0.1}_{-0.1} \text{ }^{1.1}_{-1.3}$	$11.96^{+0.09}_{-0.09} \text{ }^{1.02}_{-0.88}$	$9.91^{+0.12}_{-0.12} \text{ }^{0.95}_{-0.67}$	$5.1^{+0.3}_{-0.3} \text{ }^{1.0}_{-0.8}$
[6000, 7000]	$8.45^{+0.14}_{-0.14} \text{ }^{0.79}_{-0.94}$	$7.83^{+0.07}_{-0.07} \text{ }^{0.64}_{-0.73}$	$6.33^{+0.06}_{-0.06} \text{ }^{0.50}_{-0.49}$	$4.44^{+0.08}_{-0.08} \text{ }^{0.35}_{-0.35}$	$1.93^{+0.32}_{-0.32} \text{ }^{0.40}_{-0.36}$
[7000, 8000]	$4.96^{+0.09}_{-0.09} \text{ }^{0.46}_{-0.54}$	$4.25^{+0.05}_{-0.05} \text{ }^{0.37}_{-0.41}$	$3.70^{+0.05}_{-0.05} \text{ }^{0.32}_{-0.27}$	$2.68^{+0.07}_{-0.07} \text{ }^{0.30}_{-0.27}$	
[8000, 9000]	$2.91^{+0.06}_{-0.06} \text{ }^{0.28}_{-0.32}$	$2.53^{+0.04}_{-0.04} \text{ }^{0.22}_{-0.23}$	$2.08^{+0.04}_{-0.04} \text{ }^{0.21}_{-0.15}$	$1.19^{+0.06}_{-0.06} \text{ }^{0.21}_{-0.15}$	
[9000, 10000]	$1.26^{+0.03}_{-0.03} \text{ }^{0.12}_{-0.13}$	$1.59^{+0.03}_{-0.03} \text{ }^{0.14}_{-0.14}$	$1.23^{+0.03}_{-0.03} \text{ }^{0.10}_{-0.09}$	$0.92^{+0.08}_{-0.08} \text{ }^{0.15}_{-0.12}$	
[10000, 11000]	$1.17^{+0.04}_{-0.04} \text{ }^{0.10}_{-0.11}$	$1.034^{+0.025}_{-0.025} \text{ }^{0.089}_{-0.083}$	$0.830^{+0.025}_{-0.025} \text{ }^{0.066}_{-0.048}$	$0.382^{+0.067}_{-0.067} \text{ }^{0.079}_{-0.067}$	
[11000, 12000]	$0.721^{+0.027}_{-0.027} \text{ }^{0.065}_{-0.069}$	$0.661^{+0.020}_{-0.020} \text{ }^{0.061}_{-0.052}$	$0.472^{+0.021}_{-0.021} \text{ }^{0.046}_{-0.033}$		
[12000, 13000]	$0.494^{+0.023}_{-0.023} \text{ }^{0.048}_{-0.047}$	$0.491^{+0.017}_{-0.017} \text{ }^{0.047}_{-0.036}$	$0.347^{+0.021}_{-0.021} \text{ }^{0.030}_{-0.022}$		
[13000, 14000]	$0.374^{+0.020}_{-0.020} \text{ }^{0.043}_{-0.037}$	$0.292^{+0.014}_{-0.014} \text{ }^{0.031}_{-0.021}$	$0.272^{+0.022}_{-0.022} \text{ }^{0.033}_{-0.020}$		
[14000, 15000]	$0.218^{+0.015}_{-0.015} \text{ }^{0.034}_{-0.024}$	$0.248^{+0.014}_{-0.014} \text{ }^{0.026}_{-0.016}$	$0.110^{+0.016}_{-0.016} \text{ }^{0.023}_{-0.017}$		

Table 8. Differential production cross-sections, $d^2\sigma/(dp_T dy)$, in $\mu\text{b}/(\text{GeV}/c)$ for prompt $D^{*+} + D^{*-}$ mesons in bins of (p_T, y) . The first uncertainty is statistical, and the second is the total systematic.

p_T [MeV/c]	y				
	[2, 2.5]	[2.5, 3]	[3, 3.5]	[3.5, 4]	[4, 4.5]
[0, 1000]	$1.12^{+0.06+0.19}_{-0.05-0.15}$	$1.44^{+0.05+0.18}_{-0.05-0.17}$	$1.54^{+0.07+0.18}_{-0.06-0.14}$	$1.59^{+0.09+0.18}_{-0.08-0.14}$	$1.80^{+0.19+0.24}_{-0.15-0.18}$
[1000, 2000]	$1.40^{+0.06+0.21}_{-0.05-0.17}$	$1.48^{+0.04+0.17}_{-0.04-0.15}$	$1.61^{+0.05+0.17}_{-0.05-0.15}$	$1.67^{+0.07+0.18}_{-0.06-0.15}$	$1.85^{+0.13+0.22}_{-0.11-0.17}$
[2000, 3000]	$1.53^{+0.06+0.18}_{-0.05-0.18}$	$1.65^{+0.04+0.19}_{-0.04-0.15}$	$1.83^{+0.05+0.20}_{-0.05-0.16}$	$1.86^{+0.07+0.21}_{-0.06-0.16}$	$2.00^{+0.14+0.25}_{-0.12-0.20}$
[3000, 4000]	$1.62^{+0.07+0.20}_{-0.07-0.18}$	$1.92^{+0.06+0.21}_{-0.06-0.17}$	$1.84^{+0.06+0.20}_{-0.06-0.16}$	$2.25^{+0.10+0.29}_{-0.10-0.22}$	$2.32^{+0.21+0.35}_{-0.18-0.26}$
[4000, 5000]	$1.79^{+0.10+0.24}_{-0.09-0.18}$	$2.00^{+0.09+0.25}_{-0.08-0.19}$	$1.90^{+0.09+0.21}_{-0.08-0.16}$	$2.32^{+0.16+0.28}_{-0.14-0.23}$	$2.30^{+0.41+0.51}_{-0.31-0.31}$
[5000, 6000]	$1.90^{+0.14+0.26}_{-0.13-0.19}$	$1.78^{+0.10+0.23}_{-0.09-0.17}$	$2.18^{+0.15+0.28}_{-0.14-0.22}$	$2.14^{+0.21+0.29}_{-0.17-0.20}$	$1.69^{+0.73+0.72}_{-0.40-0.29}$
[6000, 7000]	$1.88^{+0.22+0.27}_{-0.18-0.18}$	$2.00^{+0.19+0.27}_{-0.16-0.20}$	$2.41^{+0.30+0.32}_{-0.24-0.25}$	$2.19^{+0.38+0.37}_{-0.28-0.25}$	
[7000, 8000]	$2.17^{+0.48+0.39}_{-0.33-0.22}$	$2.01^{+0.36+0.32}_{-0.26-0.19}$	$3.15^{+0.87+0.51}_{-0.56-0.33}$	$2.16^{+0.95+0.67}_{-0.51-0.30}$	

Table 9. The ratios of differential production cross-sections, $R_{13/7}$, for prompt $D^0 + \bar{D}^0$ mesons in bins of (p_T, y) . The first uncertainty is statistical, and the second is the total systematic.

p_T [MeV/c]	y				
	[2, 2.5]	[2.5, 3]	[3, 3.5]	[3.5, 4]	[4, 4.5]
[0, 1000]		$1.85^{+0.16}_{-0.14} + 0.66 - 0.43$	$1.57^{+0.10}_{-0.09} + 0.46 - 0.31$	$1.66^{+0.13}_{-0.11} + 0.48 - 0.33$	$1.50^{+0.23}_{-0.19} + 0.62 - 0.38$
[1000, 2000]	$1.48^{+0.21}_{-0.16} + 0.52 - 0.32$	$1.51^{+0.07}_{-0.06} + 0.43 - 0.26$	$1.66^{+0.06}_{-0.05} + 0.36 - 0.27$	$1.61^{+0.06}_{-0.06} + 0.38 - 0.26$	$1.86^{+0.15}_{-0.13} + 0.53 - 0.33$
[2000, 3000]	$1.65^{+0.14}_{-0.12} + 0.42 - 0.30$	$1.73^{+0.06}_{-0.06} + 0.38 - 0.27$	$1.71^{+0.05}_{-0.05} + 0.32 - 0.25$	$1.83^{+0.07}_{-0.06} + 0.37 - 0.26$	$2.09^{+0.17}_{-0.14} + 0.64 - 0.39$
[3000, 4000]	$1.75^{+0.13}_{-0.11} + 0.40 - 0.31$	$1.80^{+0.07}_{-0.06} + 0.33 - 0.27$	$1.87^{+0.07}_{-0.06} + 0.32 - 0.24$	$2.04^{+0.09}_{-0.09} + 0.40 - 0.28$	$2.47^{+0.26}_{-0.21} + 0.74 - 0.44$
[4000, 5000]	$2.01^{+0.16}_{-0.14} + 0.42 - 0.34$	$1.90^{+0.09}_{-0.08} + 0.32 - 0.26$	$1.98^{+0.10}_{-0.09} + 0.35 - 0.24$	$2.34^{+0.16}_{-0.14} + 0.52 - 0.33$	$3.00^{+0.48}_{-0.37} + 0.93 - 0.54$
[5000, 6000]	$2.24^{+0.23}_{-0.19} + 0.52 - 0.40$	$2.07^{+0.13}_{-0.12} + 0.38 - 0.28$	$2.17^{+0.15}_{-0.13} + 0.38 - 0.26$	$2.48^{+0.23}_{-0.19} + 0.57 - 0.36$	$5.4^{+2.1}_{-1.2} + 2.2 - 0.9$
[6000, 7000]	$2.16^{+0.27}_{-0.21} + 0.49 - 0.35$	$2.14^{+0.19}_{-0.16} + 0.38 - 0.27$	$1.74^{+0.15}_{-0.13} + 0.48 - 0.29$	$3.06^{+0.43}_{-0.34} + 0.88 - 0.53$	
[7000, 8000]	$2.04^{+0.33}_{-0.25} + 0.53 - 0.33$	$2.26^{+0.30}_{-0.24} + 0.45 - 0.28$	$2.51^{+0.37}_{-0.28} + 0.76 - 0.40$	$4.0^{+1.1}_{-0.7} + 1.4 - 0.7$	

Table 10. The ratios of differential production cross-sections, $R_{13/7}$, for prompt $D^+ + D^-$ mesons in bins of (p_T, y) . The first uncertainty is statistical, and the second is the total systematic.

p_T [MeV/c]	y				
	[2, 2.5]	[2.5, 3]	[3, 3.5]	[3.5, 4]	[4, 4.5]
[1000, 2000]	$0.86^{+0.47+0.61}_{-0.23-0.24}$	$1.51^{+0.28+0.63}_{-0.21-0.31}$	$2.74^{+0.60+0.97}_{-0.41-0.53}$	$2.6^{+1.0+1.3}_{-0.6-0.5}$	
[2000, 3000]	$3.6^{+1.6+1.9}_{-0.8-0.8}$	$2.89^{+0.47+0.76}_{-0.35-0.46}$	$2.28^{+0.29+0.56}_{-0.24-0.35}$	$2.76^{+0.60+0.79}_{-0.42-0.43}$	$2.1^{+1.3+1.0}_{-0.6-0.4}$
[3000, 4000]	$3.6^{+1.4+1.5}_{-0.8-0.7}$	$2.29^{+0.34+0.55}_{-0.27-0.38}$	$2.41^{+0.40+0.69}_{-0.30-0.37}$	$2.55^{+0.55+0.73}_{-0.39-0.38}$	$2.9^{+2.2+1.3}_{-0.9-0.5}$
[4000, 5000]	$3.5^{+1.3+1.3}_{-0.8-0.6}$	$3.08^{+0.63+0.77}_{-0.45-0.44}$	$3.61^{+0.87+0.94}_{-0.59-0.48}$	$2.96^{+0.93+0.84}_{-0.57-0.43}$	
[5000, 6000]	$4.2^{+2.5+1.8}_{-1.1-0.8}$	$3.21^{+0.88+0.98}_{-0.58-0.44}$	$3.3^{+1.0+0.9}_{-0.7-0.4}$	$3.4^{+1.6+1.5}_{-0.8-0.5}$	
[6000, 7000]	$2.8^{+1.4+1.2}_{-0.7-0.5}$	$3.8^{+1.7+1.2}_{-0.9-0.5}$	$2.44^{+1.00+0.78}_{-0.55-0.33}$		
[7000, 8000]	$2.0^{+1.1+1.1}_{-0.5-0.4}$		$3.4^{+2.5+1.4}_{-1.0-0.5}$		

Table 11. The ratios of differential production cross-sections, $R_{13/7}$, for prompt $D_s^+ + D_s^-$ mesons in bins of (p_T, y) . The first uncertainty is statistical, and the second is the total systematic.

p_T [MeV/c]	y				
	[2, 2.5]	[2.5, 3]	[3, 3.5]	[3.5, 4]	[4, 4.5]
[0, 1000]					$0.71^{+0.30+0.33}_{-0.18-0.20}$
[1000, 2000]		$1.13^{+0.18+0.24}_{-0.13-0.16}$	$1.53^{+0.10+0.25}_{-0.09-0.21}$	$1.58^{+0.14+0.27}_{-0.12-0.22}$	$1.75^{+0.28+0.39}_{-0.21-0.22}$
[2000, 3000]		$1.75^{+0.18+0.34}_{-0.15-0.22}$	$2.02^{+0.13+0.33}_{-0.12-0.26}$	$1.72^{+0.14+0.30}_{-0.12-0.21}$	$1.65^{+0.24+0.33}_{-0.19-0.22}$
[3000, 4000]	$1.82^{+0.46+0.40}_{-0.31-0.28}$	$1.67^{+0.14+0.28}_{-0.12-0.23}$	$1.76^{+0.13+0.32}_{-0.11-0.20}$	$1.89^{+0.18+0.37}_{-0.15-0.24}$	$2.77^{+0.72+0.65}_{-0.48-0.35}$
[4000, 5000]	$1.43^{+0.28+0.29}_{-0.20-0.22}$	$2.21^{+0.26+0.39}_{-0.21-0.31}$	$1.85^{+0.19+0.34}_{-0.16-0.22}$	$2.11^{+0.28+0.42}_{-0.22-0.27}$	$1.71^{+0.74+0.53}_{-0.39-0.23}$
[5000, 6000]	$1.83^{+0.50+0.37}_{-0.32-0.26}$	$1.80^{+0.25+0.32}_{-0.20-0.25}$	$1.74^{+0.24+0.35}_{-0.19-0.22}$	$2.53^{+0.55+0.59}_{-0.39-0.27}$	
[6000, 7000]	$1.76^{+0.57+0.40}_{-0.35-0.26}$	$2.20^{+0.48+0.46}_{-0.34-0.30}$	$3.02^{+0.94+0.77}_{-0.58-0.36}$	$3.3^{+1.8+0.9}_{-0.8-0.4}$	
[7000, 8000]	$1.42^{+0.71+0.42}_{-0.36-0.22}$	$1.93^{+0.76+0.50}_{-0.42-0.26}$			

Table 12. The ratios of differential production cross-sections, $R_{13/7}$, for prompt $D^{*+} + D^{*-}$ mesons in bins of (p_T, y) . The first uncertainty is statistical, and the second is the total systematic.

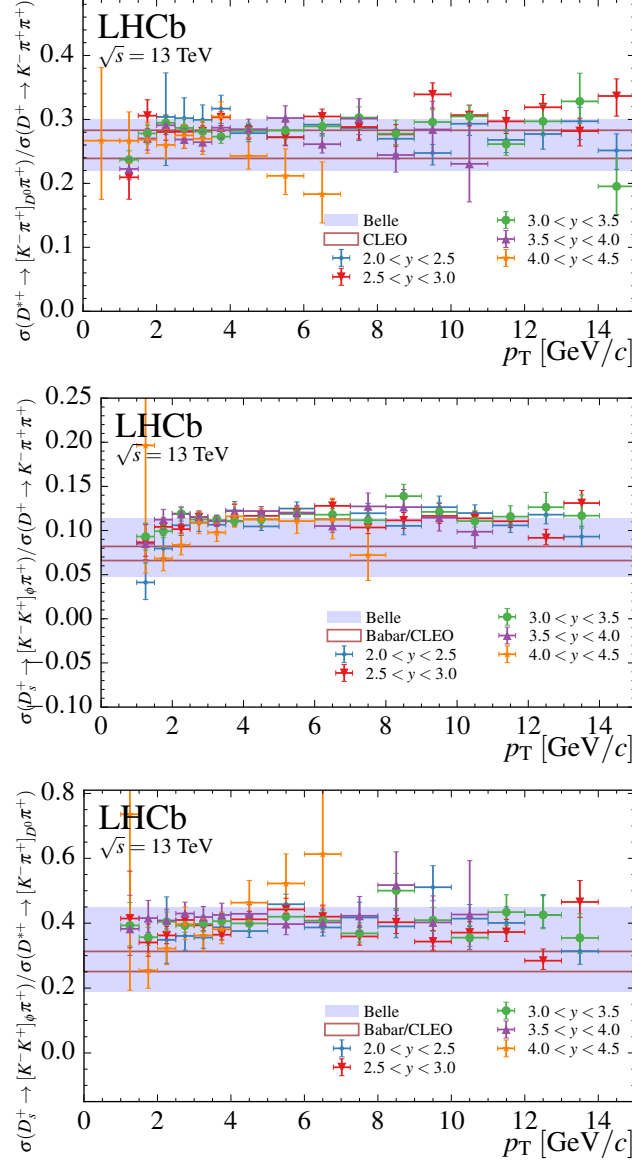


Figure 10. Ratios of cross-section-times-branching-fraction measurements of (top) D^{*+} , and (middle) D_s^+ mesons with respect to D^+ cross-sections, and (bottom) D_s^+ over D^{*+} mesons. The bands indicate the corresponding ratios computed using measurements from e^+e^- collider experiments [39–41]. The ratios are given as a function of p_T and different symbols indicate different ranges in y . The notation $\sigma(D \rightarrow f)$ is shorthand for $\sigma(D) \times \mathcal{B}(D \rightarrow f)$.

p_T [MeV/c]	y				
	[2, 2.5]	[2.5, 3]	[3, 3.5]	[3.5, 4]	[4, 4.5]
[0, 1000]		$132 \pm 5 \pm 29$	$89 \pm 2 \pm 10$	$89 \pm 3 \pm 10$	$82 \pm 5 \pm 17$
[1000, 1500]	$99 \pm 4 \pm 20$	$87.3 \pm 0.9 \pm 11.8$	$95.5 \pm 0.8 \pm 6.3$	$91.1 \pm 1.0 \pm 5.9$	$95.8 \pm 2.1 \pm 9.2$
[1500, 2000]	$88.3 \pm 1.5 \pm 9.9$	$86.1 \pm 0.5 \pm 8.5$	$95.1 \pm 0.5 \pm 4.8$	$91.3 \pm 0.6 \pm 4.6$	$95.2 \pm 1.4 \pm 6.8$
[2000, 2500]	$88.0 \pm 1.0 \pm 8.8$	$94.4 \pm 0.5 \pm 7.4$	$92.9 \pm 0.4 \pm 3.7$	$88.4 \pm 0.5 \pm 3.9$	$98.0 \pm 1.2 \pm 6.0$
[2500, 3000]	$88.8 \pm 0.9 \pm 8.2$	$96.6 \pm 0.5 \pm 4.5$	$94.1 \pm 0.4 \pm 3.5$	$96.9 \pm 0.6 \pm 4.0$	$96.6 \pm 1.2 \pm 5.8$
[3000, 3500]	$90.9 \pm 0.9 \pm 8.1$	$100.5 \pm 0.5 \pm 4.5$	$101.6 \pm 0.5 \pm 3.7$	$96.3 \pm 0.6 \pm 4.2$	$96.1 \pm 1.4 \pm 6.0$
[3500, 4000]	$91.0 \pm 0.9 \pm 7.2$	$98.4 \pm 0.5 \pm 4.6$	$105.7 \pm 0.6 \pm 4.2$	$94.8 \pm 0.7 \pm 4.3$	$91.8 \pm 1.5 \pm 7.2$
[4000, 5000]	$103.2 \pm 0.8 \pm 5.9$	$103.0 \pm 0.5 \pm 4.3$	$100.9 \pm 0.5 \pm 4.0$	$98.9 \pm 0.7 \pm 4.6$	$125 \pm 2 \pm 13$
[5000, 6000]	$100.2 \pm 0.9 \pm 4.9$	$108.2 \pm 0.6 \pm 4.6$	$105.6 \pm 0.7 \pm 4.7$	$106.6 \pm 1.0 \pm 4.6$	$149 \pm 6 \pm 26$
[6000, 7000]	$106.0 \pm 1.1 \pm 5.5$	$101.1 \pm 0.8 \pm 4.5$	$103.0 \pm 0.9 \pm 5.1$	$112.8 \pm 1.6 \pm 7.7$	$210 \pm 40 \pm 130$
[7000, 8000]	$115.5 \pm 1.6 \pm 6.9$	$102.8 \pm 1.0 \pm 4.7$	$104.8 \pm 1.2 \pm 6.1$	$122 \pm 3 \pm 12$	
[8000, 9000]	$119.5 \pm 2.0 \pm 8.5$	$108.2 \pm 1.4 \pm 5.6$	$113.0 \pm 1.7 \pm 7.2$	$114 \pm 5 \pm 17$	
[9000, 10000]	$87.8 \pm 1.8 \pm 4.8$	$91.0 \pm 1.5 \pm 3.5$	$102.0 \pm 2.1 \pm 3.2$	$143 \pm 12 \pm 24$	
[10000, 11000]	$108.4 \pm 2.7 \pm 5.3$	$104.7 \pm 2.2 \pm 2.7$	$113.7 \pm 3.2 \pm 4.2$	$146 \pm 32 \pm 32$	
[11000, 12000]	$114.9 \pm 3.6 \pm 5.5$	$101.4 \pm 2.7 \pm 2.6$	$119.3 \pm 4.9 \pm 4.8$		
[12000, 13000]	$119.2 \pm 4.6 \pm 7.2$	$101.0 \pm 3.4 \pm 2.8$	$110.4 \pm 6.3 \pm 6.8$		
[13000, 14000]	$114.2 \pm 5.3 \pm 6.6$	$97.8 \pm 4.0 \pm 4.2$	$125 \pm 10 \pm 15$		
[14000, 15000]	$118.1 \pm 6.9 \pm 7.2$	$100.9 \pm 5.2 \pm 5.9$	$142 \pm 20 \pm 25$		

Table 13. The ratios of differential production cross-section-times-branching fraction measurements for prompt D^+ and D^0 mesons in bins of (p_T , y). The first uncertainty is statistical, and the second is the total systematic. All values are given in percent.

p_T [MeV/c]	y				
	[2, 2.5]	[2.5, 3]	[3, 3.5]	[3.5, 4]	[4, 4.5]
[1000, 1500]	$4.1^{+1.0}_{-1.0} \pm 1.8$	$7.6^{+0.5}_{-0.5} \pm 2.3$	$8.9^{+0.5}_{-0.5} \pm 1.4$	$7.7^{+0.8}_{-0.8} \pm 1.9$	$19^{+6}_{-6} \pm 5$
[1500, 2000]	$7.0^{+0.4}_{-0.4} \pm 1.5$	$9.0^{+0.2}_{-0.2} \pm 1.5$	$9.43^{+0.24}_{-0.24} \pm 0.72$	$10.3^{+0.4}_{-0.4} \pm 1.0$	$6.5^{+0.7}_{-0.7} \pm 1.1$
[2000, 2500]	$9.3^{+0.3}_{-0.3} \pm 1.6$	$9.59^{+0.17}_{-0.17} \pm 0.99$	$11.07^{+0.19}_{-0.19} \pm 0.66$	$10.50^{+0.25}_{-0.25} \pm 0.71$	$8.2^{+0.5}_{-0.5} \pm 1.1$
[2500, 3000]	$9.7^{+0.3}_{-0.3} \pm 1.4$	$11.12^{+0.16}_{-0.16} \pm 0.58$	$10.59^{+0.15}_{-0.15} \pm 0.61$	$11.19^{+0.22}_{-0.22} \pm 0.65$	$10.6^{+0.5}_{-0.5} \pm 1.1$
[3000, 3500]	$9.7^{+0.3}_{-0.3} \pm 1.2$	$11.13^{+0.16}_{-0.16} \pm 0.57$	$11.36^{+0.17}_{-0.17} \pm 0.51$	$10.66^{+0.22}_{-0.22} \pm 0.62$	$9.40^{+0.46}_{-0.46} \pm 0.96$
[3500, 4000]	$11.2^{+0.3}_{-0.3} \pm 1.2$	$10.88^{+0.17}_{-0.17} \pm 0.55$	$11.72^{+0.19}_{-0.19} \pm 0.60$	$11.58^{+0.25}_{-0.25} \pm 0.73$	$10.6^{+0.6}_{-0.6} \pm 1.3$
[4000, 5000]	$10.80^{+0.22}_{-0.21} \pm 0.90$	$12.01^{+0.15}_{-0.15} \pm 0.60$	$11.37^{+0.15}_{-0.15} \pm 0.48$	$12.08^{+0.22}_{-0.22} \pm 0.57$	$14.0^{+0.7}_{-0.7} \pm 2.1$
[5000, 6000]	$12.5^{+0.3}_{-0.3} \pm 1.2$	$13.02^{+0.21}_{-0.20} \pm 0.77$	$12.53^{+0.22}_{-0.22} \pm 0.65$	$12.79^{+0.30}_{-0.29} \pm 0.88$	$16.5^{+1.2}_{-1.2} \pm 2.8$
[6000, 7000]	$11.95^{+0.33}_{-0.33} \pm 0.81$	$12.94^{+0.27}_{-0.26} \pm 0.77$	$12.15^{+0.28}_{-0.27} \pm 0.73$	$11.86^{+0.40}_{-0.39} \pm 0.96$	$23^{+5}_{-4} \pm 10$
[7000, 8000]	$13.8^{+0.5}_{-0.5} \pm 1.2$	$10.64^{+0.29}_{-0.29} \pm 0.58$	$11.71^{+0.35}_{-0.34} \pm 0.94$	$15.5^{+0.8}_{-0.8} \pm 2.2$	
[8000, 9000]	$12.6^{+0.5}_{-0.5} \pm 1.1$	$12.06^{+0.41}_{-0.41} \pm 0.84$	$15.7^{+0.6}_{-0.6} \pm 1.2$	$14.5^{+1.1}_{-1.1} \pm 3.0$	
[9000, 10000]	$11.11^{+0.56}_{-0.55} \pm 0.96$	$10.60^{+0.46}_{-0.45} \pm 0.57$	$12.35^{+0.61}_{-0.59} \pm 0.79$	$16.3^{+2.1}_{-1.9} \pm 3.7$	
[10000, 11000]	$12.84^{+0.80}_{-0.78} \pm 0.82$	$11.92^{+0.63}_{-0.63} \pm 0.24$	$12.30^{+0.82}_{-0.82} \pm 0.77$	$14.5^{+4.1}_{-3.2} \pm 4.8$	
[11000, 12000]	$12.05^{+0.94}_{-0.94} \pm 0.69$	$11.21^{+0.74}_{-0.74} \pm 0.42$	$13.5^{+1.1}_{-1.1} \pm 1.0$		
[12000, 13000]	$14.0^{+1.2}_{-1.2} \pm 0.9$	$9.17^{+0.81}_{-0.80} \pm 0.43$	$14.0^{+1.5}_{-1.4} \pm 1.0$		
[13000, 14000]	$10.6^{+1.3}_{-1.2} \pm 0.6$	$12.8^{+1.2}_{-1.1} \pm 0.8$	$14.1^{+2.2}_{-2.0} \pm 1.9$		
[14000, 15000]					

Table 14. The ratios of differential production cross-section-times-branching-fraction measurements for prompt D_s^+ and D^0 mesons in bins of (p_T, y) . The first uncertainty is statistical, and the second is the total systematic. All values are given in percent.

p_T [MeV/c]	y			
	[2, 2.5]	[2.5, 3]	[3, 3.5]	[3.5, 4]
[0, 1000]				$21.9^{+3.0+6.7}_{-3.0-6.3}$
[1000, 1500]		$18.3^{+0.8+2.0}_{-0.8-2.0}$	$22.6^{+0.3+1.3}_{-0.3-1.6}$	$20.3^{+0.3+1.4}_{-0.3-1.5}$
[1500, 2000]		$26.3^{+0.4+1.6}_{-0.4-1.6}$	$26.4^{+0.2+1.3}_{-0.2-1.9}$	$24.7^{+0.3+1.5}_{-0.3-1.9}$
[2000, 2500]	$26.8^{+2.4+5.7}_{-2.4-6.0}$	$26.5^{+0.3+1.9}_{-0.3-1.1}$	$27.4^{+0.2+1.3}_{-0.2-1.8}$	$25.5^{+0.6+2.5}_{-0.6-2.0}$
[2500, 3000]	$26.8^{+0.9+2.9}_{-0.9-3.1}$	$27.1^{+0.3+1.2}_{-0.3-1.7}$	$27.0^{+0.2+1.6}_{-0.2-1.5}$	$26.6^{+0.6+1.8}_{-0.6-2.0}$
[3000, 3500]	$27.2^{+0.7+2.2}_{-0.7-2.5}$	$28.3^{+0.2+1.2}_{-0.2-1.9}$	$28.6^{+0.2+1.7}_{-0.2-1.4}$	$25.5^{+0.3+1.8}_{-0.3-1.8}$
[3500, 4000]	$28.9^{+0.6+2.1}_{-0.6-2.5}$	$29.8^{+0.3+1.4}_{-0.3-2.1}$	$28.9^{+0.2+1.8}_{-0.2-1.4}$	$27.9^{+0.8+2.7}_{-0.8-2.7}$
[4000, 5000]	$28.8^{+0.4+1.4}_{-0.4-2.3}$	$29.2^{+0.2+1.3}_{-0.2-2.0}$	$28.5^{+0.2+1.6}_{-0.2-1.4}$	$30.3^{+0.9+2.3}_{-0.9-2.2}$
[5000, 6000]	$27.3^{+0.4+1.3}_{-0.4-2.3}$	$29.4^{+0.2+1.4}_{-0.2-2.0}$	$29.9^{+0.3+1.7}_{-0.3-1.3}$	$32.2^{+0.4+2.3}_{-0.5-1.6}$
[6000, 7000]	$30.9^{+0.5+1.8}_{-0.5-2.6}$	$30.8^{+0.3+1.6}_{-0.3-2.1}$	$29.8^{+0.4+1.7}_{-0.4-1.5}$	$29.5^{+0.6+2.2}_{-0.6-2.2}$
[7000, 8000]	$33.1^{+0.7+2.0}_{-0.7-2.9}$	$29.6^{+0.4+1.7}_{-0.4-2.3}$	$31.7^{+0.5+2.2}_{-0.5-1.6}$	$36.8^{+1.3+4.4}_{-1.2-4.3}$
[8000, 9000]	$32.2^{+0.8+2.2}_{-0.8-2.9}$	$29.9^{+0.5+1.9}_{-0.5-2.3}$	$31.4^{+0.7+2.8}_{-0.7-1.7}$	$28.0^{+1.8+4.1}_{-1.7-3.4}$
[9000, 10000]	$21.8^{+0.7+1.2}_{-0.7-1.7}$	$30.9^{+0.7+1.6}_{-0.7-2.1}$	$30.2^{+0.8+1.6}_{-0.8-1.5}$	$40.6^{+4.8+6.1}_{-4.3-7.0}$
[10000, 11000]	$31.8^{+1.2+1.6}_{-1.1-2.2}$	$32.1^{+0.9+1.6}_{-0.9-2.1}$	$34.6^{+1.4+1.8}_{-1.3-1.8}$	34^{+10+13}_{-8-11}
[11000, 12000]	$30.8^{+1.3+1.6}_{-1.4-2.5}$	$30.1^{+1.1+1.4}_{-1.1-2.0}$	$31.2^{+1.8+1.6}_{-1.7-1.7}$	
[12000, 13000]	$33.0^{+1.8+2.1}_{-1.8-3.1}$	$32.2^{+1.4+1.6}_{-1.4-2.2}$	$32.8^{+2.5+2.2}_{-2.4-1.8}$	
[13000, 14000]	$34.0^{+2.1+1.8}_{-2.1-3.0}$	$27.6^{+1.6+1.5}_{-1.6-2.0}$	$41.2^{+4.7+3.1}_{-4.3-3.4}$	
[14000, 15000]	$29.7^{+2.5+1.9}_{-2.4-2.4}$	$34.0^{+2.5+2.3}_{-2.3-2.5}$	$27.8^{+5.6+6.7}_{-4.8-5.7}$	

Table 15. The ratios of differential production cross-section-times-branching-fraction measurements for prompt D^{*+} and D^0 mesons in bins of (p_T , y). The first uncertainty is statistical, and the second is the total systematic. All values are given in percent.

p_T [MeV/c]	y				
	[2, 2.5]	[2.5, 3]	[3, 3.5]	[3.5, 4]	[4, 4.5]
[1000, 1500]	$4.1^{+1.0}_{-1.0} \pm 2.0$	$8.7^{+0.6}_{-0.6} \pm 1.9$	$9.3^{+0.6}_{-0.6} \pm 1.4$	$8.5^{+0.8}_{-0.8} \pm 2.0$	$20^{+6}_{-6} \pm 5$
[1500, 2000]	$8.0^{+0.5}_{-0.5} \pm 1.5$	$10.42^{+0.28}_{-0.28} \pm 0.98$	$9.92^{+0.25}_{-0.25} \pm 0.68$	$11.2^{+0.4}_{-0.4} \pm 1.1$	$6.8^{+0.7}_{-0.7} \pm 1.2$
[2000, 2500]	$10.6^{+0.4}_{-0.4} \pm 1.4$	$10.15^{+0.18}_{-0.18} \pm 0.58$	$11.93^{+0.20}_{-0.20} \pm 0.56$	$11.88^{+0.28}_{-0.28} \pm 0.76$	$8.4^{+0.5}_{-0.5} \pm 1.1$
[2500, 3000]	$10.9^{+0.3}_{-0.3} \pm 1.2$	$11.51^{+0.17}_{-0.17} \pm 0.44$	$11.25^{+0.17}_{-0.16} \pm 0.60$	$11.55^{+0.23}_{-0.23} \pm 0.65$	$10.9^{+0.5}_{-0.5} \pm 1.1$
[3000, 3500]	$10.66^{+0.30}_{-0.29} \pm 0.93$	$11.07^{+0.16}_{-0.17} \pm 0.42$	$11.18^{+0.17}_{-0.17} \pm 0.56$	$11.07^{+0.22}_{-0.22} \pm 0.59$	$9.77^{+0.48}_{-0.48} \pm 0.93$
[3500, 4000]	$12.27^{+0.33}_{-0.33} \pm 0.95$	$11.05^{+0.17}_{-0.17} \pm 0.43$	$11.09^{+0.18}_{-0.18} \pm 0.54$	$12.21^{+0.27}_{-0.26} \pm 0.69$	$11.6^{+0.6}_{-0.6} \pm 1.3$
[4000, 5000]	$10.47^{+0.21}_{-0.21} \pm 0.66$	$11.66^{+0.15}_{-0.15} \pm 0.46$	$11.27^{+0.15}_{-0.15} \pm 0.42$	$12.21^{+0.22}_{-0.22} \pm 0.45$	$11.2^{+0.5}_{-0.5} \pm 1.1$
[5000, 6000]	$12.49^{+0.29}_{-0.29} \pm 0.70$	$12.03^{+0.19}_{-0.19} \pm 0.62$	$11.87^{+0.20}_{-0.20} \pm 0.51$	$12.00^{+0.28}_{-0.27} \pm 0.81$	$11.1^{+0.7}_{-0.7} \pm 1.4$
[6000, 7000]	$11.28^{+0.31}_{-0.31} \pm 0.71$	$12.80^{+0.26}_{-0.26} \pm 0.70$	$11.80^{+0.27}_{-0.27} \pm 0.62$	$10.51^{+0.34}_{-0.33} \pm 0.99$	$11.2^{+1.3}_{-1.3} \pm 2.0$
[7000, 8000]	$12.0^{+0.4}_{-0.4} \pm 1.0$	$10.35^{+0.28}_{-0.27} \pm 0.58$	$11.17^{+0.33}_{-0.33} \pm 0.74$	$12.7^{+0.6}_{-0.6} \pm 1.4$	$7.2^{+2.0}_{-1.9} \pm 2.7$
[8000, 9000]	$10.53^{+0.43}_{-0.44} \pm 0.98$	$11.15^{+0.38}_{-0.38} \pm 0.81$	$13.9^{+0.5}_{-0.5} \pm 1.2$	$12.7^{+0.9}_{-0.8} \pm 1.8$	
[9000, 10000]	$12.6^{+0.6}_{-0.6} \pm 1.1$	$11.65^{+0.49}_{-0.50} \pm 0.76$	$12.11^{+0.58}_{-0.58} \pm 0.92$	$11.4^{+1.1}_{-1.1} \pm 1.2$	
[10000, 11000]	$11.98^{+0.72}_{-0.72} \pm 0.37$	$11.38^{+0.59}_{-0.61} \pm 0.43$	$11.07^{+0.70}_{-0.71} \pm 0.60$	$9.9^{+1.8}_{-1.7} \pm 1.1$	
[11000, 12000]	$10.58^{+0.80}_{-0.81} \pm 0.36$	$11.05^{+0.73}_{-0.71} \pm 0.52$	$11.57^{+0.89}_{-0.89} \pm 0.45$		
[12000, 13000]	$11.8^{+1.0}_{-1.0} \pm 0.6$	$9.17^{+0.79}_{-0.78} \pm 0.38$	$12.6^{+1.2}_{-1.2} \pm 0.6$		
[13000, 14000]	$9.3^{+1.1}_{-1.1} \pm 0.4$	$13.1^{+1.2}_{-1.2} \pm 0.8$	$11.7^{+1.6}_{-1.6} \pm 1.1$		
[14000, 15000]					

Table 16. The ratios of differential production cross-section-times-branching-fraction measurements for prompt D_s^+ and D^+ mesons in bins of (p_T, y) . The first uncertainty is statistical, and the second is the total systematic. All values are given in percent.

p_T [MeV/c]	y				
	[2, 2.5]	[2.5, 3]	[3, 3.5]	[3.5, 4]	[4, 4.5]
[0, 1000]					$27^{+4}_{-4} +^{11}_{-8}$
[1000, 1500]		$20.9^{+0.9+2.5}_{-0.9-3.3}$	$23.7^{+0.3+1.4}_{-0.4-1.6}$	$22.3^{+0.4+1.5}_{-0.4-1.6}$	$26.7^{+1.0+4.4}_{-1.0-3.4}$
[1500, 2000]		$30.6^{+0.5+2.4}_{-0.5-2.8}$	$27.8^{+0.2+1.3}_{-0.2-1.6}$	$27.0^{+0.3+1.5}_{-0.3-1.8}$	$26.8^{+0.7+2.7}_{-0.6-2.0}$
[2000, 2500]	$30.4^{+2.8+6.3}_{-2.7-7.1}$	$28.0^{+0.3+1.7}_{-0.3-1.2}$	$29.5^{+0.2+1.2}_{-0.2-1.4}$	$29.1^{+0.3+1.6}_{-0.3-1.4}$	$26.0^{+0.5+2.4}_{-0.5-2.1}$
[2500, 3000]	$30.2^{+1.1+3.0}_{-1.1-3.5}$	$28.1^{+0.3+1.0}_{-0.3-1.0}$	$28.7^{+0.2+1.5}_{-0.2-1.1}$	$26.9^{+0.3+1.6}_{-0.3-1.4}$	$27.5^{+0.6+1.6}_{-0.6-1.9}$
[3000, 3500]	$29.9^{+0.8+2.2}_{-0.8-2.6}$	$28.1^{+0.2+0.8}_{-0.3-1.0}$	$28.1^{+0.2+1.5}_{-0.2-1.0}$	$26.4^{+0.3+1.6}_{-0.3-1.4}$	$27.0^{+0.6+2.8}_{-0.6-2.4}$
[3500, 4000]	$31.7^{+0.7+2.0}_{-0.7-2.2}$	$30.3^{+0.3+0.8}_{-0.3-1.2}$	$27.3^{+0.2+1.4}_{-0.2-1.0}$	$28.7^{+0.3+1.7}_{-0.3-1.6}$	$30.4^{+0.8+2.1}_{-0.8-2.0}$
[4000, 5000]	$27.9^{+0.4+1.3}_{-0.4-1.3}$	$28.3^{+0.2+0.7}_{-0.2-1.2}$	$28.2^{+0.2+1.2}_{-0.2-1.1}$	$28.5^{+0.3+1.6}_{-0.3-1.6}$	$24.3^{+0.7+2.7}_{-0.7-1.9}$
[5000, 6000]	$27.2^{+0.4+1.2}_{-0.4-1.2}$	$27.2^{+0.2+0.8}_{-0.2-1.3}$	$28.3^{+0.2+1.3}_{-0.2-1.3}$	$30.2^{+0.4+1.9}_{-0.4-1.3}$	$21.2^{+1.2+4.0}_{-1.2-2.7}$
[6000, 7000]	$29.2^{+0.5+1.4}_{-0.5-1.5}$	$30.5^{+0.3+1.1}_{-0.3-1.6}$	$28.9^{+0.3+1.2}_{-0.3-1.5}$	$26.1^{+0.5+1.6}_{-0.5-1.3}$	$18.3^{+3.0+4.0}_{-3.0-3.4}$
[7000, 8000]	$28.7^{+0.6+1.4}_{-0.6-1.9}$	$28.8^{+0.4+1.4}_{-0.4-1.8}$	$30.3^{+0.5+1.6}_{-0.5-1.6}$	$30.1^{+0.9+3.0}_{-0.9-2.3}$	
[8000, 9000]	$27.0^{+0.7+1.4}_{-0.7-2.2}$	$27.7^{+0.5+1.4}_{-0.5-1.8}$	$27.8^{+0.6+2.1}_{-0.5-1.6}$	$24.4^{+1.2+3.8}_{-1.2-2.4}$	
[9000, 10000]	$24.7^{+0.8+1.1}_{-0.8-1.7}$	$33.9^{+0.7+1.7}_{-0.7-2.0}$	$29.6^{+0.8+1.7}_{-0.8-1.3}$	$28.4^{+2.6+3.6}_{-2.5-2.8}$	
[10000, 11000]	$29.3^{+1.0+0.6}_{-1.0-1.5}$	$30.7^{+0.8+1.3}_{-0.8-1.5}$	$30.5^{+1.1+1.4}_{-1.0-0.3}$	$23.1^{+4.2+4.8}_{-4.1-4.3}$	
[11000, 12000]	$26.8^{+1.2+0.8}_{-1.1-1.6}$	$29.7^{+1.0+1.3}_{-1.0-1.6}$	$26.1^{+1.3+1.9}_{-1.3-1.2}$		
[12000, 13000]	$27.7^{+1.4+1.0}_{-1.4-1.9}$	$31.9^{+1.3+1.5}_{-1.3-1.7}$	$29.7^{+2.0+1.7}_{-2.0-1.1}$		
[13000, 14000]	$29.7^{+1.8+1.2}_{-1.7-2.3}$	$28.2^{+1.6+1.3}_{-1.5-1.8}$	$32.8^{+3.0+3.2}_{-2.8-2.0}$		
[14000, 15000]	$25.1^{+2.0+1.7}_{-1.9-2.2}$	$33.7^{+2.2+1.6}_{-2.1-2.4}$	$19.5^{+3.0+3.2}_{-2.9-3.3}$		

Table 17. The ratios of differential production cross-section-times-branching-fraction for prompt D^{*+} and D^+ mesons in bins of (p_T, y) . The first uncertainty is statistical, and the second is the total systematic. All values are given in percent.

p_T [MeV/c]	y				
	[2, 2.5]	[2.5, 3]	[3, 3.5]	[3.5, 4]	[4, 4.5]
[1000, 1500]		$41 \pm 3 \pm 14$ $-3 -8$	$39.3 \pm 2.4 \pm 6.6$ $-2.4 -5.8$	$38.3 \pm 3.9 \pm 9.6$ $-3.8 -7.2$	$74 \pm 24 \pm 22$ $-24 -49$
[1500, 2000]		$34.1 \pm 1.1 \pm 5.6$ $-1.0 -4.1$	$35.7 \pm 0.9 \pm 2.9$ $-0.9 -2.4$	$41.6 \pm 1.5 \pm 5.2$ $-1.3 -4.1$	$25.4 \pm 2.7 \pm 4.6$ $-2.6 -4.8$
[2000, 2500]	$35 \pm 4 \pm 13$ $-3 -7$	$36.2 \pm 0.7 \pm 2.7$ $-0.7 -2.5$	$40.5 \pm 0.7 \pm 2.9$ $-0.7 -2.1$	$40.8 \pm 1.0 \pm 3.3$ $-1.0 -3.3$	$32.2 \pm 2.2 \pm 5.0$ $-2.2 -4.5$
[2500, 3000]	$36.1 \pm 1.7 \pm 6.7$ $-1.6 -4.1$	$41.0 \pm 0.7 \pm 1.8$ $-0.7 -2.1$	$39.3 \pm 0.6 \pm 2.6$ $-0.6 -2.0$	$43.0 \pm 0.9 \pm 3.4$ $-0.9 -3.4$	$39.7 \pm 2.1 \pm 4.8$ $-2.1 -4.2$
[3000, 3500]	$35.6 \pm 1.3 \pm 4.9$ $-1.3 -3.1$	$39.4 \pm 0.7 \pm 1.8$ $-0.6 -1.6$	$39.8 \pm 0.6 \pm 2.3$ $-0.6 -2.3$	$41.9 \pm 0.9 \pm 3.1$ $-0.9 -3.2$	$36.2 \pm 1.9 \pm 4.7$ $-1.9 -4.5$
[3500, 4000]	$38.7 \pm 1.3 \pm 4.1$ $-1.3 -2.6$	$36.4 \pm 0.6 \pm 1.9$ $-0.6 -1.3$	$40.6 \pm 0.7 \pm 2.4$ $-0.7 -2.5$	$42.5 \pm 1.0 \pm 3.5$ $-1.0 -3.3$	$38.1 \pm 2.3 \pm 4.8$ $-2.3 -3.8$
[4000, 5000]	$37.6 \pm 0.9 \pm 2.8$ $-0.9 -1.8$	$41.2 \pm 0.6 \pm 2.4$ $-0.6 -1.2$	$39.9 \pm 0.6 \pm 2.1$ $-0.6 -2.2$	$42.9 \pm 0.8 \pm 2.7$ $-0.8 -3.0$	$46.3 \pm 2.4 \pm 6.4$ $-2.3 -5.2$
[5000, 6000]	$45.8 \pm 1.2 \pm 2.9$ $-1.2 -2.7$	$44.2 \pm 0.8 \pm 3.4$ $-0.8 -1.5$	$42.0 \pm 0.8 \pm 2.5$ $-0.8 -2.4$	$39.7 \pm 1.0 \pm 3.1$ $-1.0 -3.1$	$52.2 \pm 4.6 \pm 7.9$ $-4.2 -7.8$
[6000, 7000]	$38.7 \pm 1.2 \pm 2.9$ $-1.2 -2.3$	$42.0 \pm 0.9 \pm 3.4$ $-0.9 -2.0$	$40.8 \pm 1.0 \pm 2.9$ $-1.0 -2.5$	$40.2 \pm 1.5 \pm 3.8$ $-1.4 -2.6$	$61 \pm 14 \pm 19$ $-11 -12$
[7000, 8000]	$41.7 \pm 1.6 \pm 4.5$ $-1.6 -2.6$	$35.9 \pm 1.0 \pm 3.1$ $-1.0 -2.5$	$36.9 \pm 1.2 \pm 3.0$ $-1.1 -2.5$	$42.3 \pm 2.3 \pm 5.5$ $-2.2 -4.2$	
[8000, 9000]	$39.0 \pm 1.8 \pm 4.6$ $-1.7 -3.1$	$40.3 \pm 1.5 \pm 3.9$ $-1.4 -3.2$	$50.0 \pm 2.0 \pm 4.9$ $-2.0 -5.1$	$51.8 \pm 4.2 \pm 9.3$ $-4.0 -8.5$	
[9000, 10000]	$51.1 \pm 2.8 \pm 6.0$ $-2.8 -3.1$	$34.3 \pm 1.5 \pm 3.1$ $-1.5 -2.2$	$40.9 \pm 2.1 \pm 3.4$ $-2.1 -2.8$	$40.2 \pm 5.5 \pm 6.1$ $-4.8 -5.5$	
[10000, 11000]	$41.4 \pm 2.7 \pm 2.1$ $-2.7 -2.1$	$37.1 \pm 2.1 \pm 2.6$ $-2.1 -1.6$	$35.5 \pm 2.5 \pm 2.8$ $-2.5 -1.2$	$43 \pm 12 \pm 11$ $-9 -5$	
[11000, 12000]	$40.1 \pm 3.3 \pm 2.4$ $-3.2 -2.4$	$37.3 \pm 2.6 \pm 3.0$ $-2.6 -1.3$	$43.4 \pm 3.9 \pm 3.7$ $-3.7 -1.7$		
[12000, 13000]	$42.5 \pm 4.1 \pm 4.3$ $-3.8 -1.2$	$28.4 \pm 2.6 \pm 2.5$ $-2.5 -0.9$	$42.6 \pm 4.7 \pm 2.5$ $-4.6 -2.5$		
[13000, 14000]	$31.4 \pm 4.0 \pm 3.3$ $-3.9 -1.0$	$46.5 \pm 4.7 \pm 4.7$ $-4.5 -1.5$	$35.5 \pm 5.5 \pm 2.8$ $-5.4 -2.7$		
[14000, 15000]					

Table 18. The ratios of differential production cross-section-times-branching-fraction for prompt D_s^+ and D^{*+} mesons in bins of (p_T, y) . The first uncertainty is statistical, and the second is the total systematic. All values are given in percent.

Open Access. This article is distributed under the terms of the Creative Commons Attribution License ([CC-BY 4.0](https://creativecommons.org/licenses/by/4.0/)), which permits any use, distribution and reproduction in any medium, provided the original author(s) and source are credited.

References

- [1] LHCb collaboration, *Measurements of prompt charm production cross-sections in pp collisions at $\sqrt{s} = 13$ TeV*, *JHEP* **03** (2016) 159 [Erratum *ibid.* **09** (2016) 013] [[arXiv:1510.01707](https://arxiv.org/abs/1510.01707)] [[INSPIRE](#)].
- [2] A. Affolder et al., *Radiation damage in the LHCb vertex locator*, *2013 JINST* **8** P08002 [[arXiv:1302.5259](https://arxiv.org/abs/1302.5259)] [[INSPIRE](#)].
- [3] LHCb collaboration, *Measurement of the track reconstruction efficiency at LHCb*, *2015 JINST* **10** P02007 [[arXiv:1408.1251](https://arxiv.org/abs/1408.1251)] [[INSPIRE](#)].

The LHCb collaboration

R. Aaij³⁸, C. Abellán Beteta⁴⁰, B. Adeva³⁷, M. Adinolfi⁴⁶, A. Affolder⁵², Z. Ajaltouni⁵, S. Akar⁶, J. Albrecht⁹, F. Alessio³⁸, M. Alexander⁵¹, S. Ali⁴¹, G. Alkhazov³⁰, P. Alvarez Cartelle⁵³, A.A. Alves Jr⁵⁷, S. Amato², S. Amerio²², Y. Amhis⁷, L. An³, L. Anderlini¹⁷, J. Anderson⁴⁰, G. Andreassi³⁹, M. Andreotti^{16,f}, J.E. Andrews⁵⁸, R.B. Appleby⁵⁴, O. Aquines Gutierrez¹⁰, F. Archilli³⁸, P. d'Argent¹¹, A. Artamonov³⁵, M. Artuso⁵⁹, E. Aslanides⁶, G. Auriemma^{25,m}, M. Baalouch⁵, S. Bachmann¹¹, J.J. Back⁴⁸, A. Badalov³⁶, C. Baesso⁶⁰, W. Baldini^{16,38}, R.J. Barlow⁵⁴, C. Barschel³⁸, S. Barsuk⁷, W. Barter³⁸, V. Batozskaya²⁸, V. Battista³⁹, A. Bay³⁹, L. Beaucourt⁴, J. Beddow⁵¹, F. Bedeschi²³, I. Bediaga¹, L.J. Bel⁴¹, V. Bellee³⁹, N. Belloli^{20,j}, I. Belyaev³¹, E. Ben-Haim⁸, G. Bencivenni¹⁸, S. Benson³⁸, J. Benton⁴⁶, A. Berezhnoy³², R. Bernet⁴⁰, A. Bertolin²², M.-O. Bettler³⁸, M. van Beuzekom⁴¹, A. Bien¹¹, S. Bifani⁴⁵, P. Billoir⁸, T. Bird⁵⁴, A. Birnkraut⁹, A. Bizzeti^{17,h}, T. Blake⁴⁸, F. Blanc³⁹, J. Blouw¹⁰, S. Blusk⁵⁹, V. Bocci²⁵, A. Bondar³⁴, N. Bondar^{30,38}, W. Bonivento¹⁵, S. Borghi⁵⁴, M. Borsato⁷, T.J.V. Bowcock⁵², E. Bowen⁴⁰, C. Bozzi¹⁶, S. Braun¹¹, M. Britsch¹⁰, T. Britton⁵⁹, J. Brodzicka⁵⁴, N.H. Brook⁴⁶, E. Buchanan⁴⁶, C. Burr^{49,54}, A. Bursche⁴⁰, J. Buytaert³⁸, S. Cadeddu¹⁵, R. Calabrese^{16,f}, M. Calvi^{20,j}, M. Calvo Gomez^{36,o}, P. Campana¹⁸, D. Campora Perez³⁸, L. Capriotti⁵⁴, A. Carbone^{14,d}, G. Carboni^{24,k}, R. Cardinale^{19,i}, A. Cardini¹⁵, P. Carniti^{20,j}, L. Carson⁵⁰, K. Carvalho Akiba^{2,38}, G. Casse⁵², L. Cassina^{20,j}, L. Castillo Garcia³⁸, M. Cattaneo³⁸, Ch. Cauet⁹, G. Cavallero¹⁹, R. Cenci^{23,s}, M. Charles⁸, Ph. Charpentier³⁸, M. Chefdeville⁴, S. Chen⁵⁴, S.-F. Cheung⁵⁵, N. Chiapolini⁴⁰, M. Chrzasczcz⁴⁰, X. Cid Vidal³⁸, G. Ciezarek⁴¹, P.E.L. Clarke⁵⁰, M. Clemencic³⁸, H.V. Cliff⁴⁷, J. Closier³⁸, V. Coco³⁸, J. Cogan⁶, E. Cogneras⁵, V. Cogoni^{15,e}, L. Cojocariu²⁹, G. Collazuol²², P. Collins³⁸, A. Comerma-Montells¹¹, A. Contu¹⁵, A. Cook⁴⁶, M. Coombes⁴⁶, S. Coquereau⁸, G. Corti³⁸, M. Corvo^{16,f}, B. Couturier³⁸, G.A. Cowan⁵⁰, D.C. Craik⁴⁸, A. Crocombe⁴⁸, M. Cruz Torres⁶⁰, S. Cunliffe⁵³, R. Currie⁵³, C. D'Ambrosio³⁸, E. Dall'Occo⁴¹, J. Dalseno⁴⁶, P.N.Y. David⁴¹, A. Davis⁵⁷, O. De Aguiar Francisco², K. De Bruyn⁶, S. De Capua⁵⁴, M. De Cian¹¹, J.M. De Miranda¹, L. De Paula², P. De Simone¹⁸, C.-T. Dean⁵¹, D. Decamp⁴, M. Deckenhoff⁹, L. Del Buono⁸, N. Déleage⁴, M. Demmer⁹, D. Derkach⁶⁵, O. Deschamps⁵, F. Dettori³⁸, B. Dey²¹, A. Di Canto³⁸, F. Di Ruscio²⁴, H. Dijkstra³⁸, S. Donleavy⁵², F. Dordei¹¹, M. Dorigo³⁹, A. Dosil Suárez³⁷, D. Dossett⁴⁸, A. Dovbnya⁴³, K. Dreimanis⁵², L. Dufour⁴¹, G. Dujany⁵⁴, F. Dupertuis³⁹, P. Durante³⁸, R. Dzhelezhyan³⁵, A. Dziurda²⁶, A. Dzyuba³⁰, S. Easo^{49,38}, U. Egede⁵³, V. Egorychev³¹, S. Eidelman³⁴, S. Eisenhardt⁵⁰, U. Eitschberger⁹, R. Ekelhof⁹, L. Eklund⁵¹, I. El Rifai⁵, Ch. Elsasser⁴⁰, S. Ely⁵⁹, S. Esen¹¹, H.M. Evans⁴⁷, T. Evans⁵⁵, A. Falabella¹⁴, C. Färber³⁸, N. Farley⁴⁵, S. Farry⁵², R. Fay⁵², D. Ferguson⁵⁰, V. Fernandez Albor³⁷, F. Ferrari¹⁴, F. Ferreira Rodrigues¹, M. Ferro-Luzzi³⁸, S. Filippov³³, M. Fiore^{16,38,f}, M. Fiorini^{16,f}, M. Firlej²⁷, C. Fitzpatrick³⁹, T. Fiutowski²⁷, K. Fohl³⁸, P. Fol⁵³, M. Fontana¹⁵, F. Fontanelli^{19,i}, D. C. Forshaw⁵⁹, R. Forty³⁸, M. Frank³⁸, C. Frei³⁸, M. Frosini¹⁷, J. Fu²¹, E. Furfaro^{24,k}, A. Gallas Torreira³⁷, D. Galli^{14,d}, S. Gallorini²², S. Gambetta⁵⁰, M. Gandelman², P. Gandini⁵⁵, Y. Gao³, J. García Pardiñas³⁷, J. Garra Tico⁴⁷, L. Garrido³⁶, D. Gascon³⁶, C. Gaspar³⁸, R. Gauld⁵⁵, L. Gavardi⁹, G. Gazzoni⁵, D. Gerick¹¹, E. Gersabeck¹¹, M. Gersabeck⁵⁴, T. Gershon⁴⁸, Ph. Ghez⁴, S. Gianì³⁹, V. Gibson⁴⁷, O.G. Girard³⁹, L. Giubega²⁹, V.V. Gligorov³⁸, C. Göbel⁶⁰, D. Golubkov³¹, A. Golutvin^{53,38}, A. Gomes^{1,a}, C. Gotti^{20,j}, M. Grabalosa Gándara⁵, R. Graciani Diaz³⁶, L.A. Granado Cardoso³⁸, E. Graugés³⁶, E. Graverini⁴⁰, G. Graziani¹⁷, A. Grecu²⁹, E. Greening⁵⁵, S. Gregson⁴⁷, P. Griffith⁴⁵, L. Grillo¹¹, O. Grünberg⁶³, B. Gui⁵⁹, E. Gushchin³³, Yu. Guz^{35,38}, T. Gys³⁸, T. Hadavizadeh⁵⁵, C. Hadjivasiliou⁵⁹, G. Haefeli³⁹, C. Haen³⁸, S.C. Haines⁴⁷, S. Hall⁵³, B. Hamilton⁵⁸, X. Han¹¹, S. Hansmann-Menzemer¹¹, N. Harnew⁵⁵, S.T. Harnew⁴⁶, J. Harrison⁵⁴, J. He³⁸, T. Head³⁹, V. Heijne⁴¹, K. Hennessy⁵²,

P. Henrard⁵, L. Henry⁸, E. van Herwijnen³⁸, M. Heß⁶³, A. Hicheur², D. Hill⁵⁵, M. Hoballah⁵, C. Hombach⁵⁴, W. Hulsbergen⁴¹, T. Humair⁵³, N. Hussain⁵⁵, D. Hutchcroft⁵², D. Hynds⁵¹, M. Idzik²⁷, P. Ilten⁵⁶, R. Jacobsson³⁸, A. Jaeger¹¹, J. Jalocha⁵⁵, E. Jans⁴¹, A. Jawahery⁵⁸, F. Jing³, M. John⁵⁵, D. Johnson³⁸, C.R. Jones⁴⁷, C. Joram³⁸, B. Jost³⁸, N. Jurik⁵⁹, S. Kandybei⁴³, W. Kanso⁶, M. Karacson³⁸, T.M. Karbach^{38,†}, S. Karodia⁵¹, M. Kecke¹¹, M. Kelsey⁵⁹, I.R. Kenyon⁴⁵, M. Kenzie³⁸, T. Ketel⁴², E. Khairullin⁶⁵, B. Khanji^{20,38,j}, C. Khurewathanakul³⁹, S. Klaver⁵⁴, K. Klimaszewski²⁸, O. Kochebina⁷, M. Kolpin¹¹, I. Komarov³⁹, R.F. Koopman⁴², P. Koppenburg^{41,38}, M. Kozeiha⁵, L. Kravchuk³³, K. Kreplin¹¹, M. Krepes⁴⁸, G. Krocker¹¹, P. Krokovny³⁴, F. Kruse⁹, W. Krzemien²⁸, W. Kucewicz^{26,n}, M. Kucharczyk²⁶, V. Kudryavtsev³⁴, A. K. Kuonen³⁹, K. Kurek²⁸, T. Kvaratskheliya³¹, D. Lacarrere³⁸, G. Lafferty^{54,38}, A. Lai¹⁵, D. Lambert⁵⁰, G. Lanfranchi¹⁸, C. Langenbruch⁴⁸, B. Langhans³⁸, T. Latham⁴⁸, C. Lazzeroni⁴⁵, R. Le Gac⁶, J. van Leerdam⁴¹, J.-P. Lees⁴, R. Lefèvre⁵, A. Leflat^{32,38}, J. Lefrançois⁷, E. Lemos Cid³⁷, O. Leroy⁶, T. Lesiak²⁶, B. Leverington¹¹, Y. Li⁷, T. Likhomanenko^{65,64}, M. Liles⁵², R. Lindner³⁸, C. Linn³⁸, F. Lionetto⁴⁰, B. Liu¹⁵, X. Liu³, D. Loh⁴⁸, I. Longstaff⁵¹, J.H. Lopes², D. Lucchesi^{22,q}, M. Lucio Martinez³⁷, H. Luo⁵⁰, A. Lupato²², E. Luppi^{16,f}, O. Lupton⁵⁵, A. Lusiani²³, F. Machefert⁷, F. Maciuc²⁹, O. Maev³⁰, K. Maguire⁵⁴, S. Malde⁵⁵, A. Malinin⁶⁴, G. Manca⁷, G. Mancinelli⁶, P. Manning⁵⁹, A. Mapelli³⁸, J. Maratas⁵, J.F. Marchand⁴, U. Marconi¹⁴, C. Marin Benito³⁶, P. Marino^{23,38,s}, J. Marks¹¹, G. Martellotti²⁵, M. Martin⁶, M. Martinelli³⁹, D. Martinez Santos³⁷, F. Martinez Vidal⁶⁶, D. Martins Tostes², A. Massafferri¹, R. Matev³⁸, A. Mathad⁴⁸, Z. Mathe³⁸, C. Matteuzzi²⁰, A. Mauri⁴⁰, B. Maurin³⁹, A. Mazurov⁴⁵, M. McCann⁵³, J. McCarthy⁴⁵, A. McNab⁵⁴, R. McNulty¹², B. Meadows⁵⁷, F. Meier⁹, M. Meissner¹¹, D. Melnychuk²⁸, M. Merk⁴¹, E. Michielin²², D.A. Milanes⁶², M.-N. Minard⁴, D.S. Mitzel¹¹, J. Molina Rodriguez⁶⁰, I.A. Monroy⁶², S. Monteil⁵, M. Morandin²², P. Morawski²⁷, A. Mordà⁶, M.J. Morello^{23,s}, J. Moron²⁷, A.B. Morris⁵⁰, R. Mountain⁵⁹, F. Muheim⁵⁰, D. Müller⁵⁴, J. Müller⁹, K. Müller⁴⁰, V. Müller⁹, M. Mussini¹⁴, B. Muster³⁹, P. Naik⁴⁶, T. Nakada³⁹, R. Nandakumar⁴⁹, A. Nandi⁵⁵, I. Nasteva², M. Needham⁵⁰, N. Neri²¹, S. Neubert¹¹, N. Neufeld³⁸, M. Neuner¹¹, A.D. Nguyen³⁹, T.D. Nguyen³⁹, C. Nguyen-Mau^{39,p}, V. Niess⁵, R. Niet⁹, N. Nikitin³², T. Nikodem¹¹, A. Novoselov³⁵, D.P. O’Hanlon⁴⁸, A. Oblakowska-Mucha²⁷, V. Obraztsov³⁵, S. Ogilvy⁵¹, O. Okhrimenko⁴⁴, R. Oldeman^{15,e}, C.J.G. Onderwater⁶⁷, B. Osorio Rodrigues¹, J.M. Otalora Goicochea², A. Otto³⁸, P. Owen⁵³, A. Oyanguren⁶⁶, A. Palano^{13,c}, F. Palombo^{21,t}, M. Palutan¹⁸, J. Panman³⁸, A. Papanestis⁴⁹, M. Pappagallo⁵¹, L.L. Pappalardo^{16,f}, C. Pappenheimer⁵⁷, W. Parker⁵⁸, C. Parkes⁵⁴, G. Passaleva¹⁷, G.D. Patel⁵², M. Patel⁵³, C. Patrignani^{19,i}, A. Pearce^{54,49}, A. Pellegrino⁴¹, G. Penso^{25,l}, M. Pepe Altarelli³⁸, S. Perazzini^{14,d}, P. Perret⁵, L. Pescatore⁴⁵, K. Petridis⁴⁶, A. Petrolini^{19,i}, M. Petruzzo²¹, E. Picatoste Olloqui³⁶, B. Pietrzyk⁴, T. Pilar⁴⁸, D. Pinci²⁵, A. Pistone¹⁹, A. Piucci¹¹, S. Playfer⁵⁰, M. Plo Casasus³⁷, T. Poikela³⁸, F. Polci⁸, A. Poluektov^{48,34}, I. Polyakov³¹, E. Polcarpo², A. Popov³⁵, D. Popov^{10,38}, B. Popovici²⁹, C. Potterat², E. Price⁴⁶, J.D. Price⁵², J. Prisciandaro³⁷, A. Pritchard⁵², C. Prouve⁴⁶, V. Pugatch⁴⁴, A. Puig Navarro³⁹, G. Punzi^{23,r}, W. Qian⁴, R. Quagliani^{7,46}, B. Rachwal²⁶, J.H. Rademacker⁴⁶, M. Rama²³, M.S. Rangel², I. Raniuk⁴³, N. Rauschmayr³⁸, G. Raven⁴², F. Redi⁵³, S. Reichert⁵⁴, M.M. Reid⁴⁸, A.C. dos Reis¹, S. Ricciardi⁴⁹, S. Richards⁴⁶, M. Rihl³⁸, K. Rinnert^{52,38}, V. Rives Molina³⁶, P. Robbe^{7,38}, A.B. Rodrigues¹, E. Rodrigues⁵⁴, J.A. Rodriguez Lopez⁶², P. Rodriguez Perez⁵⁴, S. Roiser³⁸, V. Romanovsky³⁵, A. Romero Vidal³⁷, J. W. Ronayne¹², M. Rotondo²², J. Rouvinet³⁹, T. Ruf³⁸, P. Ruiz Valls⁶⁶, J.J. Saborido Silva³⁷, N. Sagidova³⁰, P. Sail⁵¹, B. Saitta^{15,e}, V. Salustino Guimaraes², C. Sanchez Mayordomo⁶⁶, B. Sanmartin Sedes³⁷, R. Santacesaria²⁵, C. Santamarina Rios³⁷, M. Santimaria¹⁸, E. Santovetti^{24,k}, A. Sarti^{18,l}, C. Satriano^{25,m}, A. Satta²⁴, D.M. Saunders⁴⁶, D. Savrina^{31,32}, M. Schiller³⁸, H. Schindler³⁸, M. Schlupp⁹,

M. Schmelling¹⁰, T. Schmelzer⁹, B. Schmidt³⁸, O. Schneider³⁹, A. Schopper³⁸, M. Schubiger³⁹, M.-H. Schune⁷, R. Schwemmer³⁸, B. Sciascia¹⁸, A. Sciubba^{25,l}, A. Semennikov³¹, N. Serra⁴⁰, J. Serrano⁶, L. Sestini²², P. Seyfert²⁰, M. Shapkin³⁵, I. Shapoval^{16,43,f}, Y. Shcheglov³⁰, T. Shears⁵², L. Shekhtman³⁴, V. Shevchenko⁶⁴, A. Shires⁹, B.G. Siddi¹⁶, R. Silva Coutinho⁴⁰, L. Silva de Oliveira², G. Simi²², M. Sirendi⁴⁷, N. Skidmore⁴⁶, T. Skwarnicki⁵⁹, E. Smith^{55,49}, E. Smith⁵³, I.T. Smith⁵⁰, J. Smith⁴⁷, M. Smith⁵⁴, H. Snoek⁴¹, M.D. Sokoloff^{57,38}, F.J.P. Soler⁵¹, F. Soomro³⁹, D. Souza⁴⁶, B. Souza De Paula², B. Spaan⁹, P. Spradlin⁵¹, S. Sridharan³⁸, F. Stagni³⁸, M. Stahl¹¹, S. Stahl³⁸, S. Stefkova⁵³, O. Steinkamp⁴⁰, O. Stenyakin³⁵, S. Stevenson⁵⁵, S. Stoica²⁹, S. Stone⁵⁹, B. Storaci⁴⁰, S. Stracka^{23,s}, M. Straticiuc²⁹, U. Straumann⁴⁰, L. Sun⁵⁷, W. Sutcliffe⁵³, K. Swientek²⁷, S. Swientek⁹, V. Syropoulos⁴², M. Szczekowski²⁸, T. Szumlak²⁷, S. T'Jampens⁴, A. Tayduganov⁶, T. Tekampe⁹, M. Teklishyn⁷, G. Tellarini^{16,f}, F. Teubert³⁸, C. Thomas⁵⁵, E. Thomas³⁸, J. van Tilburg⁴¹, V. Tisserand⁴, M. Tobin³⁹, J. Todd⁵⁷, S. Tol⁴², L. Tomassetti^{16,f}, D. Tonelli³⁸, S. Topp-Joergensen⁵⁵, N. Tori⁵⁵, E. Tournefier⁴, S. Tourneur³⁹, K. Trabelsi³⁹, M.T. Tran³⁹, M. Tresch⁴⁰, A. Trisovic³⁸, A. Tsaregorodtsev⁶, P. Tsopelas⁴¹, N. Tuning^{41,38}, A. Ukleja²⁸, A. Ustyuzhanin^{65,64}, U. Uwer¹¹, C. Vacca^{15,38,e}, V. Vagnoni¹⁴, G. Valenti¹⁴, A. Vallier⁷, R. Vazquez Gomez¹⁸, P. Vazquez Regueiro³⁷, C. Vázquez Sierra³⁷, S. Vecchi¹⁶, J.J. Velthuis⁴⁶, M. Veltri^{17,g}, G. Veneziano³⁹, M. Vesterinen¹¹, B. Viaud⁷, D. Vieira², M. Vieites Diaz³⁷, X. Vilasis-Cardona^{36,o}, V. Volkov³², A. Vollhardt⁴⁰, D. Volynskyy¹⁰, D. Voong⁴⁶, A. Vorobyev³⁰, V. Vorobyev³⁴, C. Voß⁶³, J.A. de Vries⁴¹, R. Waldi⁶³, C. Wallace⁴⁸, R. Wallace¹², J. Walsh²³, S. Wandernoth¹¹, J. Wang⁵⁹, D.R. Ward⁴⁷, N.K. Watson⁴⁵, D. Websdale⁵³, A. Weiden⁴⁰, M. Whitehead⁴⁸, G. Wilkinson^{55,38}, M. Wilkinson⁵⁹, M. Williams³⁸, M.P. Williams⁴⁵, M. Williams⁵⁶, T. Williams⁴⁵, F.F. Wilson⁴⁹, J. Wimberley⁵⁸, J. Wishahi⁹, W. Wislicki²⁸, M. Witek²⁶, G. Wormser⁷, S.A. Wotton⁴⁷, K. Wyllie³⁸, Y. Xie⁶¹, Z. Xu³⁹, Z. Yang³, J. Yu⁶¹, X. Yuan³⁴, O. Yushchenko³⁵, M. Zangoli¹⁴, M. Zavertyaev^{10,b}, L. Zhang³, Y. Zhang³, A. Zhelezov¹¹, A. Zhokhov³¹, L. Zhong³, S. Zucchelli¹⁴

¹ Centro Brasileiro de Pesquisas Físicas (CBPF), Rio de Janeiro, Brazil

² Universidade Federal do Rio de Janeiro (UFRJ), Rio de Janeiro, Brazil

³ Center for High Energy Physics, Tsinghua University, Beijing, China

⁴ LAPP, Université Savoie Mont-Blanc, CNRS/IN2P3, Annecy-Le-Vieux, France

⁵ Clermont Université, Université Blaise Pascal, CNRS/IN2P3, LPC, Clermont-Ferrand, France

⁶ CPPM, Aix-Marseille Université, CNRS/IN2P3, Marseille, France

⁷ LAL, Université Paris-Sud, CNRS/IN2P3, Orsay, France

⁸ LPNHE, Université Pierre et Marie Curie, Université Paris Diderot, CNRS/IN2P3, Paris, France

⁹ Fakultät Physik, Technische Universität Dortmund, Dortmund, Germany

¹⁰ Max-Planck-Institut für Kernphysik (MPIK), Heidelberg, Germany

¹¹ Physikalisches Institut, Ruprecht-Karls-Universität Heidelberg, Heidelberg, Germany

¹² School of Physics, University College Dublin, Dublin, Ireland

¹³ Sezione INFN di Bari, Bari, Italy

¹⁴ Sezione INFN di Bologna, Bologna, Italy

¹⁵ Sezione INFN di Cagliari, Cagliari, Italy

¹⁶ Sezione INFN di Ferrara, Ferrara, Italy

¹⁷ Sezione INFN di Firenze, Firenze, Italy

¹⁸ Laboratori Nazionali dell'INFN di Frascati, Frascati, Italy

¹⁹ Sezione INFN di Genova, Genova, Italy

²⁰ Sezione INFN di Milano Bicocca, Milano, Italy

²¹ Sezione INFN di Milano, Milano, Italy

²² Sezione INFN di Padova, Padova, Italy

²³ Sezione INFN di Pisa, Pisa, Italy

²⁴ Sezione INFN di Roma Tor Vergata, Roma, Italy

- ²⁵ *Sezione INFN di Roma La Sapienza, Roma, Italy*
- ²⁶ *Henryk Niewodniczanski Institute of Nuclear Physics Polish Academy of Sciences, Kraków, Poland*
- ²⁷ *AGH - University of Science and Technology, Faculty of Physics and Applied Computer Science, Kraków, Poland*
- ²⁸ *National Center for Nuclear Research (NCBJ), Warsaw, Poland*
- ²⁹ *Horia Hulubei National Institute of Physics and Nuclear Engineering, Bucharest-Magurele, Romania*
- ³⁰ *Petersburg Nuclear Physics Institute (PNPI), Gatchina, Russia*
- ³¹ *Institute of Theoretical and Experimental Physics (ITEP), Moscow, Russia*
- ³² *Institute of Nuclear Physics, Moscow State University (SINP MSU), Moscow, Russia*
- ³³ *Institute for Nuclear Research of the Russian Academy of Sciences (INR RAN), Moscow, Russia*
- ³⁴ *Budker Institute of Nuclear Physics (SB RAS) and Novosibirsk State University, Novosibirsk, Russia*
- ³⁵ *Institute for High Energy Physics (IHEP), Protvino, Russia*
- ³⁶ *Universitat de Barcelona, Barcelona, Spain*
- ³⁷ *Universidad de Santiago de Compostela, Santiago de Compostela, Spain*
- ³⁸ *European Organization for Nuclear Research (CERN), Geneva, Switzerland*
- ³⁹ *Ecole Polytechnique Fédérale de Lausanne (EPFL), Lausanne, Switzerland*
- ⁴⁰ *Physik-Institut, Universität Zürich, Zürich, Switzerland*
- ⁴¹ *Nikhef National Institute for Subatomic Physics, Amsterdam, The Netherlands*
- ⁴² *Nikhef National Institute for Subatomic Physics and VU University Amsterdam, Amsterdam, The Netherlands*
- ⁴³ *NSC Kharkiv Institute of Physics and Technology (NSC KIPT), Kharkiv, Ukraine*
- ⁴⁴ *Institute for Nuclear Research of the National Academy of Sciences (KINR), Kyiv, Ukraine*
- ⁴⁵ *University of Birmingham, Birmingham, United Kingdom*
- ⁴⁶ *H.H. Wills Physics Laboratory, University of Bristol, Bristol, United Kingdom*
- ⁴⁷ *Cavendish Laboratory, University of Cambridge, Cambridge, United Kingdom*
- ⁴⁸ *Department of Physics, University of Warwick, Coventry, United Kingdom*
- ⁴⁹ *STFC Rutherford Appleton Laboratory, Didcot, United Kingdom*
- ⁵⁰ *School of Physics and Astronomy, University of Edinburgh, Edinburgh, United Kingdom*
- ⁵¹ *School of Physics and Astronomy, University of Glasgow, Glasgow, United Kingdom*
- ⁵² *Oliver Lodge Laboratory, University of Liverpool, Liverpool, United Kingdom*
- ⁵³ *Imperial College London, London, United Kingdom*
- ⁵⁴ *School of Physics and Astronomy, University of Manchester, Manchester, United Kingdom*
- ⁵⁵ *Department of Physics, University of Oxford, Oxford, United Kingdom*
- ⁵⁶ *Massachusetts Institute of Technology, Cambridge, MA, United States*
- ⁵⁷ *University of Cincinnati, Cincinnati, OH, United States*
- ⁵⁸ *University of Maryland, College Park, MD, United States*
- ⁵⁹ *Syracuse University, Syracuse, NY, United States*
- ⁶⁰ *Pontifícia Universidade Católica do Rio de Janeiro (PUC-Rio), Rio de Janeiro, Brazil, associated to ²*
- ⁶¹ *Institute of Particle Physics, Central China Normal University, Wuhan, Hubei, China, associated to ³*
- ⁶² *Departamento de Física, Universidad Nacional de Colombia, Bogota, Colombia, associated to ⁸*
- ⁶³ *Institut für Physik, Universität Rostock, Rostock, Germany, associated to ¹¹*
- ⁶⁴ *National Research Centre Kurchatov Institute, Moscow, Russia, associated to ³¹*
- ⁶⁵ *Yandex School of Data Analysis, Moscow, Russia, associated to ³¹*
- ⁶⁶ *Instituto de Física Corpuscular (IFIC), Universitat de Valencia-CSIC, Valencia, Spain, associated to ³⁶*
- ⁶⁷ *Van Swinderen Institute, University of Groningen, Groningen, The Netherlands, associated to ⁴¹*
- ^a *Universidade Federal do Triângulo Mineiro (UFTM), Uberaba-MG, Brazil*

- ^b *P.N. Lebedev Physical Institute, Russian Academy of Science (LPI RAS), Moscow, Russia*
- ^c *Università di Bari, Bari, Italy*
- ^d *Università di Bologna, Bologna, Italy*
- ^e *Università di Cagliari, Cagliari, Italy*
- ^f *Università di Ferrara, Ferrara, Italy*
- ^g *Università di Urbino, Urbino, Italy*
- ^h *Università di Modena e Reggio Emilia, Modena, Italy*
- ⁱ *Università di Genova, Genova, Italy*
- ^j *Università di Milano Bicocca, Milano, Italy*
- ^k *Università di Roma Tor Vergata, Roma, Italy*
- ^l *Università di Roma La Sapienza, Roma, Italy*
- ^m *Università della Basilicata, Potenza, Italy*
- ⁿ *AGH - University of Science and Technology, Faculty of Computer Science, Electronics and Telecommunications, Kraków, Poland*
- ^o *LIFAELS, La Salle, Universitat Ramon Llull, Barcelona, Spain*
- ^p *Hanoi University of Science, Hanoi, Viet Nam*
- ^q *Università di Padova, Padova, Italy*
- ^r *Università di Pisa, Pisa, Italy*
- ^s *Scuola Normale Superiore, Pisa, Italy*
- ^t *Università degli Studi di Milano, Milano, Italy*
- [†] *Deceased*